Zoological Journal of the Linnean Society, 2018, **182**, 808–829. With 10 figures.

Phylogeny of the Neotropical genus *Gephyrocharax* (Characiformes: Characidae: Stevardiinae), with remarks on the tribe Stevardiini

JAMES A. VANEGAS-RÍOS*

Facultad de Ciencias Naturales y Museo, CONICET, UNLP, Paseo del Bosque S/N B1900FWA, La Plata, Buenos Aires, Argentina

Received 17 August 2016; revised 10 May 2017; accepted for publication 25 June 2017

Stevardiinae, which consists of 326 species and 44 genera, is a monophyletic subfamily within the family Characidae. In a recent classification of the subfamily, the tribe Stevardiini was expanded from three (*Corynopoma*, *Gephyrocharax* and *Pterobrycon*) to six genera by the addition of *Chrysobrycon*, *Hysteronotus* and *Pseudocorynopoma*. However, no morphological evidence has supported this definition of the tribe and the monophyly of *Gephyrocharax*. To address these issues, a phylogenetic study of most stevardiins focusing on *Gephyrocharax* was conducted. A data matrix including 532 characters and 213 taxa (73 stevardiines, 19 of which were stevardiins) was processed using maximum parsimony in TNT 1.5. All characters were analysed under extended implied weighting, exploring 21 *k* values. A strict consensus (comprising the most stables trees obtained) was used as the final topology. The results support the current definition of Stevardiini, as well as the monophyly of *Chrysobrycon*, *Gephyrocharax* and *Pterobrycon*. *Corynopoma* was obtained as the sister group of *Gephyrocharax*, the latter being phylogenetically diagnosed by two synapomorphies associated with caudal-fin morphology of adult males. The following interspecific relationships within *Gephyrocharax* are hypothesised: (*G. martae* ((*G. chocoensis* (*G. major* (*G. atracaudatus*, *G. intermedius*))) (*G. venezuelae* (*G. sinuensis* (*G. valencia* (*G. caucanus* (*G. melanocheir*, *G. torresi*)))))))).

ADDITIONAL KEYWORDS: caudal muscles – *Chrysobrycon* – *Corynopoma* – extended implied weighting – pouch scale – sexual dimorphism.

INTRODUCTION

Stevardiinae constitutes a monophyletic subfamily consisting of 326 valid species and 44 valid genera and is one of the most diverse and widespread groups of the family Characidae in the Neotropical region (Mirande, 2010; Thomaz *et al.*, 2015; Eschmeyer & Fong, 2017). Recently, 33 stevardiine genera have been classified in 7 monophyletic tribes (leaving out 11 *incertae sedis* genera), one of which is Stevardiini (the other tribes are Creagrutini, Diapomini, Eretmobryconini, Glandulocaudini, Hemibryconini and Xenurobryconini) (Thomaz *et al.*, 2015).

The freshwater tribe Stevardiini (=Corynopomini) was formerly defined as a monophyletic group consisting of *Corynopoma* Gill, *Gephyrocharax* Eigenmann and *Pterobrycon* Eigenmann, as part of the first morphology-based phylogenetic study of Glandulocaudinae (Weitzman & Menezes, 1998). Weitzman & Menezes (1998) proposed two synapomorphies for Stevardiini: the presence of hypertrophied *radii* confined to the posteroventral border of a pouch scale in adult males and the position of this scale on the caudal fin, extending from the region of the principal caudal-fin ray 12 to the ventral procurrent rays. Additionally, the tribe was found within a polytomy including the genera *Hysteronotus* Eigenmann, *Phenacobrycon* Eigenmann and *Pseudocorynopoma* Perugia (Weitzman & Menezes, 1998). In a recent DNA-based phylogenetic study of Stevardiinae, Thomaz *et al.* (2015) added the species *Chrysobrycon* Weitzman & Menezes, *Pseudocorynopoma* and tentatively *Hysteronotus* to Stevardiini. This new assemblage has not been diagnosed morphologically since.

The stevardiine genus *Gephyrocharax* has been recognised as the most speciose group of stevardiins

*Corresponding author. E-mail: anyelovr@fcnym.unlp.edu.ar

(Vanegas-Ríos, 2016). Species of the genus inhabit both sides of the Andean Cordilleras from the Caribbean and Pacific coastal drainages of Panama (including the Pearl Islands) across the Atrato, Cauca, Caribbean, Lago Maracaibo, Moruga-Moriquite Magdalena, San Juan, San Jorge and Sinu basins to the Orinoco and Amazon basins in Bolivia, Colombia, Trinidad and Tobago and Venezuela (Weitzman, 2003; Vanegas-Ríos *et al.*, 2013; Vanegas-Ríos, 2016). For many years, 13 valid species have been included in the genus (Weitzman, 2003; Vanegas-Ríos *et al.*, 2013) based on the characteristics presented by Eigenmann (1912), Myers in Eigenmann & Myers (1929) and Schultz (1944). Vanegas-Ríos (2016) recognised 11 valid species as part of a revision of the genus: *Gephyrocharax atracaudatus* Meek & Hildebrand, *G. caucanus* Eigenmann, *G. chocoensis* Eigenmann, *G. martae* Dahl, *G. melanocheir* Eigenmann, *G. intermedius* Meek & Hildebrand, *G. major* Myers, *G. sinuensis* Dahl, *G. torresi* Vanegas-Ríos, Azpelicueta, Mirande & Gonzales, *G. valencia* Eigenmann, and *G. venezuelae* Schultz. In that revision, the genus was diagnosed by having the second and third ventral procurrent rays of the caudal-fin hypertrophied, forming a single spur-shaped structure in adult males (Vanegas-Ríos, 2016).

To complement the taxonomic review of *Gephyrocharax* (Vanegas-Ríos, 2014, 2016), this work conducted a phylogenetic analysis of this genus, including extensive taxon sampling of stevardiines. Secondarily, remarks on the phylogenetic relationships within Stevardiinae and especially within Stevardiini are provided.

MATERIAL AND METHODS

Institutional abbreviations

Examined specimens are deposited in 33 different institutions (AMNH, ANSP, AUM, CAR, CAS, CI-FML, CIUA, CZUT-IC, FMNH, IAvH-P, ICNMHN, IMCN, INHS, IU, LACM, LBP, MBUCV, MCP, MCZ, MEPN, MHNG, MLP, MPUJ, MUSM, MZLU, NRM, ROM, STRI, UF, UIST, UMSS, USNM and UWIZM), which are abbreviated following Sabaj (2016). In the list of examined species (Supporting Information, Appendix S1), the standard length (SL) was taken point to point with digital calipers.

Histological, osteological and myological preparations

Specimens were cleared and stained (c&s) following Taylor & Dyke (1985) to observe cartilage and bones. For myological observations, specimens were dissected and subsequently stained using a 10% solution of methylene blue or a double-stained (ds) protocol following Datovo & Bockmann (2010) and Datovo & Castro (2012). To confirm the absence of gill glands in *G. intermedius*, the branchial arch of three mature males (36.0 mm SL, STRI 1200; 38.1 mm SL, ANSP 104434 and 33.3 mm SL, ANSP 99856) were processed following the histological technique described by Terán, Mangione & Mirande (2014).

Terminology

Osteological nomenclature follows Weitzman (1962) with the following modifications: vomer instead of prevomer, intercalar instead of opisthotic (Zanata & Vari, 2005), epioccipital instead of epiotic (Patterson, 1975), posterior ceratohyal instead of epihyal or posterohyal, anterior ceratohyal instead of ceratohyal or anterohyal (Nelson, 1969), mesethmoid instead of ethmoid (Fink & Fink, 1981), autopalatine instead of palatine, endopterygoid instead of mesopterygoid and supraneurals 3 instead of neural complex (Hoffmann & Britz, 2006; Datovo & Vari, 2013; Mattox, Britz & Toledo-Piza, 2014). Total vertebral counts were determined using radiographs (r) and c&s specimens. These include the first preural centrum plus the first ural centrum (PU1+U1), which were counted as one element, plus all four vertebrae of the Weberian apparatus. Pleural ribs were numbered according to the vertebral counts (i.e. the rib of the fifth vertebra corresponds to the fifth rib). Ventral procurrent rays were posteroanteriorly numbered in ascending order, with the posteriormost ray as the first ray. Myological terminology follows Winterbottom (1973) and Weitzman & Fink (1985) for caudal muscles (e.g. the common tendon of *hypaxialis* muscles or *interradialis* sections). Counts were taken according to Fink & Weitzman (1974) and Menezes & Weitzman (2009). The general classification of the Characidae follows Mirande (2010). Since the monophyly of Stevardiinae (='clade A' of Malabarba & Weitzman 2003) was well supported in different morphological and molecular studies (Javonillo *et al.*, 2010; Oliveira *et al.*, 2011; Mirande, Jerep & Vanegas-Ríos, 2013; Thomaz *et al.*, 2015), previous definitions of the subfamily by Weitzman *et al.* (2005), Menezes & Weitzman (2009) and Ferreira, Menezes & Quagio-Grassioto (2011) were not adopted in this work. The taxonomy of *Gephyrocharax* follows Vanegas-Ríos (2016). Abbreviations are given in Table 1.

Matrix of characters and sampled terminal taxa

To test the phylogenetic position of the genus within Characidae and Stevardiinae, the morphological matrix analysed by Mirande *et al.* (2013), the most recent version of the data matrix compiled by Mirande

Table 1. Morphological abbreviations

Skeleton		Musculature	
Anguloarticular	aa	Common tendon of *hypaxialis*	ct
Antorbital	an	*Epaxialis*	ep
Cleithrum	cl	*Flexor dorsalis superior*	fds
Coracoid	co	*Flexor dorsalis*	fd
Dentary	dt	*Hypaxialis*	hy
Ectopterygoid	ec	*Hypochordal longitudinalis*	hyl
Endopterygoid	en	*Interradialis*	int
Extrascapular	exs	*Lateralis superficialis*	ls
Frontal	fr		
Horizontal process	hp		
Hypural	hyp		
Infraorbital	io		
Lateral ethmoid	le		
Maxilla	mx		
Metapterygoid	mt		
Nasal	na		
Orbitosphenoid	or		
Parasphenoid	psh		
Parietal	pa		
Pelvic bone	pb		
Postcleithrum	pc		
Posterodorsal process	pdp		
Posteroventral lobe	pvl		
Posttemporal	pt		
Pouch scale	ps		
Premaxilla	pm		
Preopercle	po		
Principal caudal-fin ray	pcfr		
Pterosphenoid	pt		
Retroarticular	ra		
Rhinosphenoid	rh		
Scapula	sc		
Spur shaped-structure	sss		
Supracleithrum	sp		
Supraneural	sn		
Supraoccipital	so		
Ventral procurrent ray	vpr		

(2010) and Mirande, Aguilera & Azpelicueta (2011) for Characidae and Stevardiinae, was used as the initial data set. The character 350 (sclerotic bones) of Mirande (2010) was observed to be very variable intraspecifically in many stevardiine species and, consequently, was excluded from the cladistic analysis. The data matrix included 532 characters combining 365 of the 366 used by Mirande *et al.* (2011), 10 used by Mirande *et al.* (2013), 69 analyzed in other literature (e.g. Weitzman & Fink, 1985; Weitzman & Menezes, 1998; Ferreira *et al.*, 2011), and 88 treated as new here. Most of the 69 characters from the literature were included in the data matrix because they were used in other phylogenetic studies focused on Glandulocaudinae *sensu* Weitzman & Menezes (1998) or on other groups allied to *Gephyrocharax* or the stevardiins (Weitzman & Fink, 1985; Weitzman & Menezes, 1998; Ferreira *et al.*, 2011). Regarding the 88 new characters, they were chosen to be phylogenetically informative for the groups under study in the cladistic analysis.

All terminal taxa analysed by Mirande *et al.* (2013) were included. However, only 120 of the terminal taxa used by those authors were coded for the 157 characters added to the data matrix (see list in Supporting Information, Appendix S2), whereas the remaining 62 terminal taxa were not coded for those characters because they were irrelevant to the objectives proposed here. Scientific names of the following species analysed

by Mirande (2010) were updated based on recent reidentifications (Mirande JM, personal communication): *Acrobrycon tarijae* Fowler was replaced with *A. ipanquianus* (Cope) *sensu* Arcila, Vari & Menezes (2013); *Astyanax* cf. *eigenmanniorum* (Cope) 1 and *A.* cf. *eigenmanniorum* 2 were merged into *A.* cf. *eigenmanniorum*; *A. asuncionensis* Géry and *A.* cf. *asuncionensis* were merged into *A. lacustris* (Lütken) *sensu* Lucena & Soares (2016); *Bryconamericus rubropictus* (Berg) and *B.* cf. *rubropictus* were merged into *B. rubropictus* (Berg). In total, 213 terminal taxa were analyzed in the data matrix (73 stevardiine species), which included all *Gephyrocharax* species [*G. atracaudatus*, *G. caucanus*, *G. chocoensis*, *G. martae*, *G. melanocheir*, *G. intermedius*, *G. major*, *G. sinuensis*, *G. torresi*, *G. valencia* and *G. venezuelae*; in total, 98 specimens (r, ds and c&s) of these species were examined] and 23 terminal species (outgroups) that were not analyzed in the data matrix of Mirande *et al.* (2013). Twenty-one of these 23 terminal species are members of Glandulocaudini, Diapomini, Eretmobryconini, Xenurobryconini and the group of *incertae sedis* species *sensu* Thomaz *et al.* (2015): *Chrysobrycon eliasi* Vanegas-Ríos, Azpelicueta & Ortega; *C. hesperus* (Böhlke); *C. guahibo* Vanegas-Ríos, Urbano-Bonilla & Azpelicueta; *C. myersi* (Weitzman & Thomerson); *C. yoliae* Vanegas-Ríos, Azpelicueta & Ortega; *Corynopoma riisei* Gill; *Diapoma terofali* (Géry); *D. pyrrhopteryx* Menezes & Weitzman; *Hemibrycon plutarcoi* (Román-Valencia, Vanegas-Ríos & Ruiz-C.); *B. yokiae* Román-Valencia; *Knodus* sp.; *Landonia latidens* Eigenmann & Henn (='Landonini' *sensu* Weitzman & Menezes, 1998); *Markiana geayi* (Pellegrin); *Mimagoniates inequalis* (Eigenmann); *Phenacobrycon henni* (Eigenmann) (='Phenacobryconini' *sensu* Weitzman & Menezes, 1998); *Planaltina glandipedis* Menezes, Weitzman & Burns (before in Diapomini *sensu* Weitzman & Menezes, 1998); *Pterobrycon landoni* Eigenmann; *P. myrnae* Bussing; *Scopaeocharax rhinodus* (Böhlke); *Tyttocharax* sp. and *Xenurobrycon macropus* Myers & Miranda-Ribeiro. The species *Odontostilbe pulchra* (Gill) and *Nematobrycon lacortei* Weitzman & Fink were added as non-stevardiine outgroups. In the data matrix, *G. martae*, *L. latidens* and *P. landoni* were partly coded based on alcohol-preserved and radiographed specimens (Supporting Information, Appendix S1), and pertinent descriptions (Roberts, 1973; Bussing, 1974).

Character coding

The character states that could not be coded are indicated in the data matrix by two symbols: '?' for missing data and '–' for logically inapplicable conditions. The hierarchical qualitative states (involving the absence/presence of a structure) were broken into two binary characters. The majority of the additive multistate characters were tried as binary characters to accelerate the searches under implied weighting (IW) method, based on Mirande's (2009) approach. For counts with 'continuous' distribution, the character states were arranged into binary characters with additive ranges that represented the limit values where the taxa were taxonomically differentiated and/or the ranges where the taxa were less variable intraspecifically (further details are provided in Supporting Information, Appendix S3).

Cladistic searches

All phylogenetic searches and procedures were performed with TNT 1.5 (Goloboff, Farris & Nixon, 2008b; Goloboff & Catalano, 2016) using the IW method (Goloboff, 1993) under the maximum parsimony criterion (Hennig, 1966; Farris, 1970, 1983). This method has been widely detailed in the literature (Goloboff, 1995, 1997; Arias & Miranda-Esquivel, 2004; Goloboff *et al.*, 2008a; Goloboff, 2014).

In the cladistic analysis, the extended IW method (Goloboff, 2014), implemented in TNT with the 'xpiwe' command, was used to avoid the characters with missing data having artificially lower numbers of steps, and hence higher weights when they are optimised on most parsimonious trees. All search conditions and procedures for choosing a final phylogenetic hypothesis using the IW scheme were based on the methodology widely explained by Mirande (2009, 2010) and Mirande *et al.* (2013) and they are not treated here in detail. In total, 21 k values were explored under a set of parameters [the minimum number of steps of the most parsimonious trees, number of the most parsimonious trees, fit, average similarity index and average subtree pruning and regrafting (SPR) distances] to compare among the different optimal trees obtained at each k value. Higher simultaneous values in two of those parameters: the similarity index ('Tcomp'), a variation of distortion coefficient of Farris (1989), and the SPR distances ('Sprdiff'), were used to select the most stable trees (or k values) obtained. A strict consensus tree (the final hypothesis) was constructed from these trees as a balance between robustness and resolution. Clade supports were estimated through relative Bremer support (rbs) (searching suboptimal trees and then using only trees within absolute support) and symmetric resampling expressed as the difference in frequencies for group present/contradicted (GC) (Bremer, 1994; Goloboff *et al.*, 2003). For calculations of the GC values, the data matrix was resampled 300 times using sectorial searches and tree drifting, calculated for the most stable k value (Goloboff, 1999). Clade stabilities

were estimated as raw frequencies and frequency differences using the consensus obtained at each *k* value explored as the source. All IW searches were made using a TNT script provided by Mirande *et al.* (2013) with the following indications: 'hits = 3, search level = 7'. The stability and support measures are presented together for each node in the following order, separated by a slash: the raw frequencies, frequency differences, GC values and rbs. Cases where these measures have (artificially) negative values are indicated with a dash (–). For each character of the data matrix, the number of optimal steps (s), consistency index (ci) and retention index (ri) were calculated.

For comparative purposes, the data set was analyzed using equal weighting (EW) for all characters ('xmult = hits3 level7 rat10 drift10 plus hold 30000 bb'). A strict consensus tree was constructed from the resulting trees. The clades of this consensus that were found in agreement with the IW consensus were indicated in the final consensus topology of the Stevardiinae.

RESULTS

Matrix analysis and cladistic results

The analyzed matrix consisted of 532 characters and 213 terminal species (Supporting Information, Appendix S4). From these characters, 116 were associated with sexual dimorphism of adult males (Supporting Information, Appendix S3). Based on the Tcomp and Sprdiff values, the three most stable consensuses were those obtained from the 8th to the 10th *k* values (=10.6–12.7), which comprise nine trees ranging from 3598 to 3599 steps (Supporting Information, Appendix S5). The strict consensus obtained from these optimal trees is presented as the final tree topology (with 3601 steps and 207 nodes, Supporting Information, Appendix S6). The monophyly of *Chrysobrycon*, *Gephyrocharax*, *Pterobrycon* and Stevardiini was resolved consistently in all consensuses explored at the 21 different *k* values under IW as well as in the EW consensus (Figs 1, 2). This result was expressed at the maximum values (=100) of absolute frequencies and frequency differences (stability measures) obtained for these clades. The support measures obtained for each clade were estimated from the trees obtained at the 10th *k* value (=12.7), which is the most stable concavity explored under conditions of IW for the characters (Supporting Information, Appendices S5 and S7). The *Chrysobrycon* and *Pterobrycon* clades received higher support values (>50) than the *Gephyrocharax* clade (<50). In the stevardiin clade, a higher value was obtained in the GC value (77) than in the rbs (30). Within the *Gephyrocharax* clade, only two sister-group relationships, consisting of *G. atracaudatus* plus *G. intermedius* and *G. melanocheir* plus *G. torresi*, were recovered with high supports in both GC values and rbs (>50).

Major clades and synapomorphies

A complete list of common synapomorphies optimising on the nine trees used to construct the final consensus is presented in Supporting Information, Appendix S7. In the following section, the main clades related to the groups under study and their common synapomorphies are presented using the node numbers depicted on the tree (Figs 1, 2 and Supporting Information, Appendix S7). The respective convergences and reversals are provided only within Stevardiinae because it is the larger group of interest and importance for this work. Each common synapomorphy is accompanied by the number of optimal steps (s), consistency index (ci) and retention index (ri) (provided for all characters in Supporting Information, Appendix S8). The character numbers plus the optimised states are indicated between parentheses, that is, plesiomorphic > apomorphic.

Node 363 (76/62/0/29) Stevardiinae

Acrobrycon Eigenmann & Pearson, *Argopleura* Eigenmann, *Aulixidens* Böhlke, *Attonitus* Vari & Ortega, *Bryconamericus* Eigenmann, *Carlastyanax* Géry, *Chrysobrycon*, *Corynopoma*, *Creagrutus* Günther, *Diapoma* Cope, *Eretmobrycon* Fink, *Gephyrocharax*, *Hemibrycon* Günther, *Knodus* Eigenmann, *Landonia* Eigenmann & Henn, *Microgenys* Eigenmann, *Mimagoniates* Regan, *Phenacobrycon*, *Planaltina* Böhlke, *Piabarchus* Myers, *Piabina* Reinhardt, *Pseudocorynopoma*, *Pterobrycon*, *Scopaeocharax* Weitzman & Fink, *Tyttocharax* Fowler and *Xenurobrycon* Myers & Miranda-Ribeiro.

1. Dorsal margin of lateral ethmoids in dorsal view (21: 0 > 1): misaligned, oriented anteriorly (s = 7, ci = 0.1, ri = 0.9).
2. Ventral margin of third infraorbital (86: 1 > 0): reaching horizontal arm of preopercle (s = 30, ci = 0, ri = 0.7). Reversed in *Bryconamericus indefessus* (Mirande, Aguilera & Azpelicueta), *B. rubropictus*, *Carlastyanax aurocaudatus* (Eigenmann), *Creagrutus meridionalis* Vari & Harold, *Creagrutus taphorni* Vari & Harold, and node 391.
3. Number of teeth on inner premaxillary row (147: 1 > 0): four or fewer (s = 17, ci = 0.1, ri = 0.7). Reversed in *Bryconamericus indefessus*, *B. lethostigmus* (Gomes), *B. rubropictus*, *Chrysobrycon eliasi*, *C. hesperus*, *C. myersi*, *C. yoliae*, *Diapoma alburnus* (Hensel), *D. obi* (Casciotta, Almirón, Piálek &

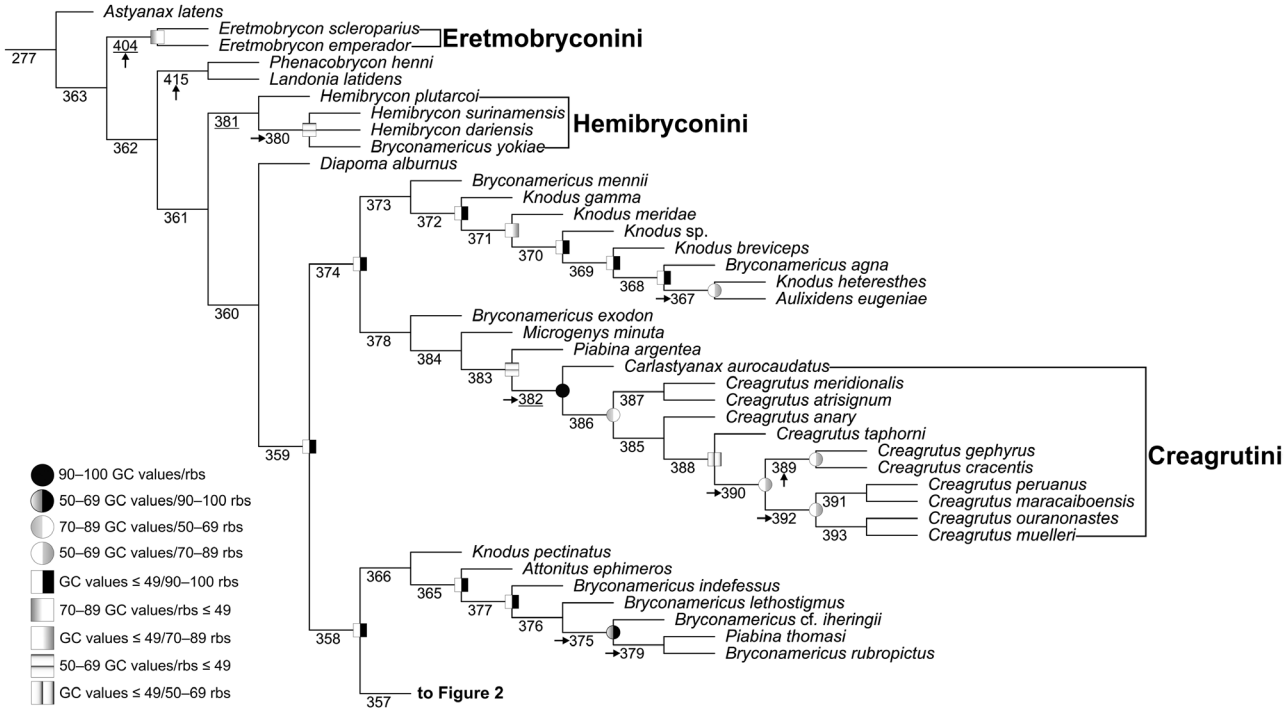

Figure 1. Final consensus topology showing the phylogenetic relationships of most stevardiines lacking hypertrophied caudal-fin squamation in adult males (Stevardiinae = node 363). Black arrows indicate common nodes obtained in the equal weighing consensus (L = 4605, ci = 0.11, ri = 0.54). Underlined node numbers represent nodes in common with Thomaz *et al.* (2015). Only higher supports are depicted on nodes: circles = GC values and relative Bremer supports (rbs) ≥50; squares = one of them ≤49. Node numbers correspond to those in the text and in Supporting Information, Appendix S7. See full tree in Supporting Information, Appendix S6.

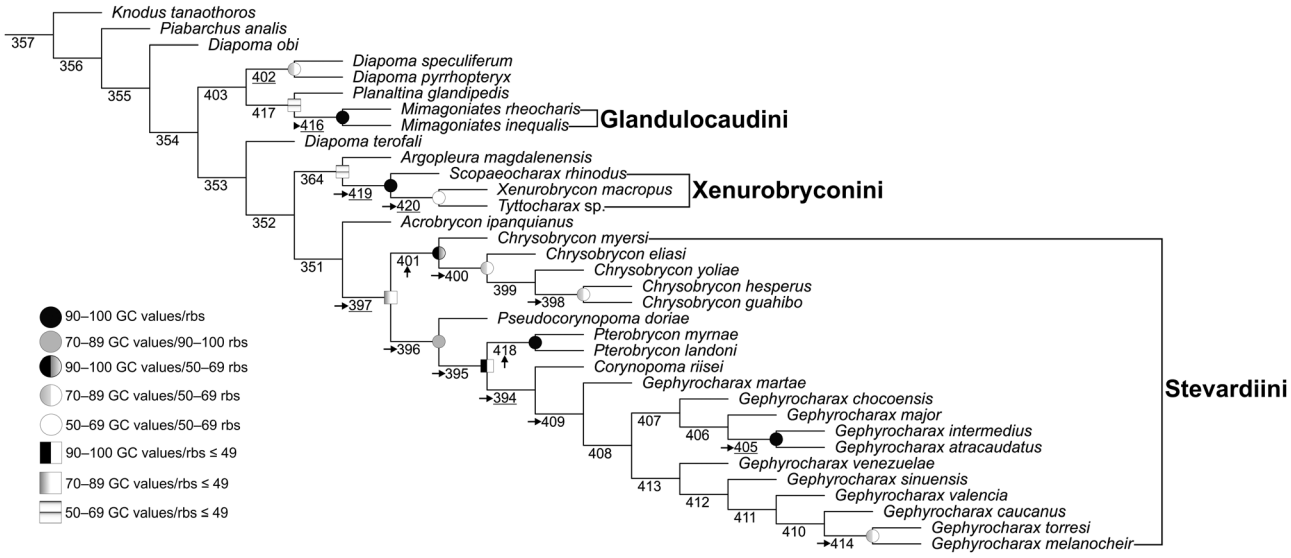

Figure 2. Final consensus topology showing the phylogenetic relationships of the *Gephyrocharax* species with remaining stevardiins (also including those stevardiines not presented in Fig. 1). Black arrows indicate common nodes obtained in the equal weighing consensus (L = 5142, ci = 0.12, ri = 0.55). Underlined node numbers represent nodes in common with Thomaz *et al.* (2015). Only higher supports are depicted on nodes: circles = GC values and relative Bremer supports (rbs) ≥50; squares = one of them ≤49. Node numbers correspond to those in the text and in Supporting Information, Appendix S7. See full tree in Supporting Information, Appendix S6.

Říčan), *D. terofali*, *D. pyrrhopteryx*, *Gephyrocharax martae*, *Hemibrycon surinamensis* Géry, and nodes 375, 391, 396, 409, 416, 417 and 419.

4. Dorsal margin of third postcleithrum (303: 0 > 1): reaching or surpassing second-postcleithrum midpoint (Fig. 3: s = 21, ci = 0.1, ri = 0.4). Reversed in *Bryconamericus indefessus*, *B. rubropictus*, *Carlastyanax aurocaudatus*, *Creagrutus anary* Fowler, *Creagrutus atrisignum* Myers, *Creagrutus meridionalis*, *Creagrutus taphorni*, *Diapoma speculiferum* Cope, *Knodus meridae* Eigenmann, *Phenacobrycon henni*, and node 382.

Node 397 (100/100/77/30) Stevardiini

1. Anterior convergence of ventral diverging lamellae with nasal septum of mesethmoid (7: 1 > 0): convergence absent or, when present, located near anterior end of nasal septum (s = 16, ci = 0.1, ri = 0.6). Reversed in *Creagrutus anary*, *C. cracentis* Vari & Harold, *C. meridionalis*, and node 361. Convergent in *Aulixidens eugeniae* Böhlke, *Bryconamericus lethostigmus*, *Carlastyanax aurocaudatus*, *Knodus breviceps* (Eigenmann), *K. pectinatus* (Vari & Siebert), *Mimagoniates inequalis*, *Piabina argentea* Reinhardt, and nodes 383, 388 and 416.

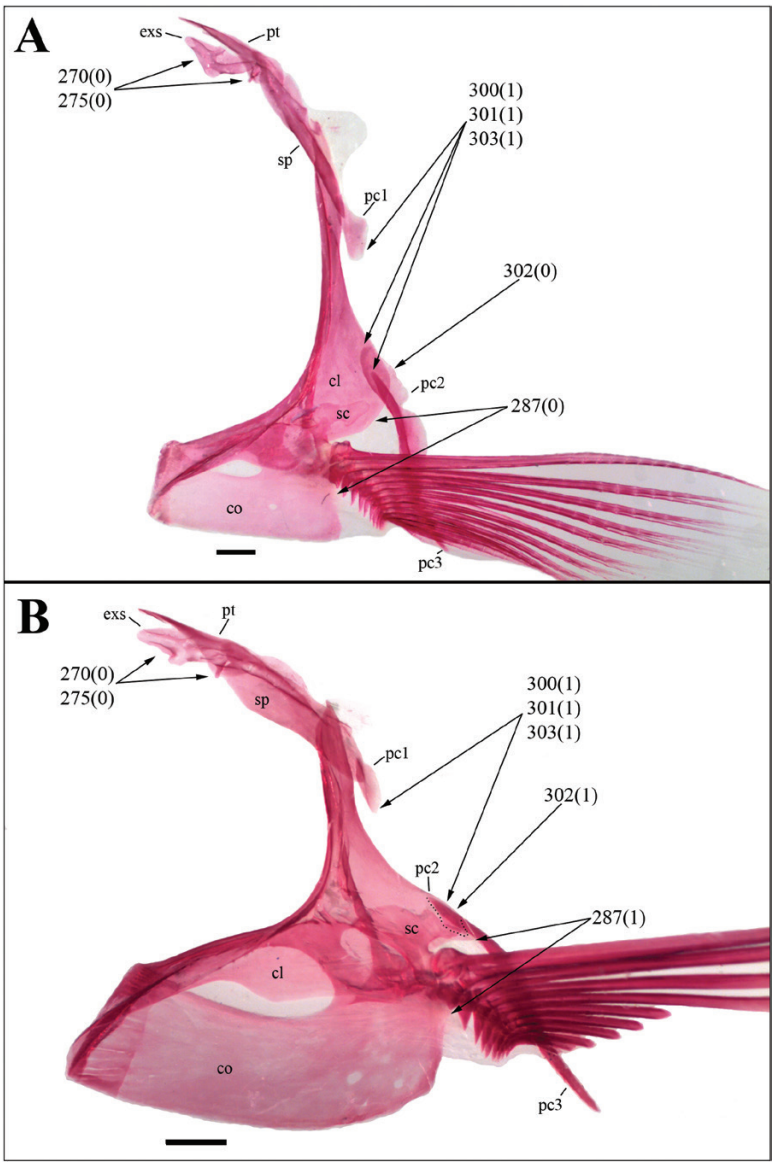

Figure 3. Pectoral girdle of *Bryconamericus yokiae* (A), male, 44.7 mm SL, MBUCV 12505, and *Gephyrocharax caucanus* (B), female, 39.8 mm SL, IMCN 3084. Arrows indicate characters analyzed in the data matrix. Abbreviations in Table 1. Left lateral view. Scale = 1 mm.

2. Parietal bone (41: 0 > 1): with its lateral border longer than its medial border (Fig. 4: states 0 and 1; s = 7, ci = 0.1, ri = 0.8). Reversed in *Gephyrocharax melanocheir*, *G. major* and *G. sinuensis* Convergent in *Knodus breviceps*, *Mimagoniates rheocharis* Menezes & Weitzman, and node 402.
3. Anterior tip of premaxilla (99: 0 > 1): horizontally aligned with upper half of orbit (Fig. 5: states 0 and 1; s = 23, ci = 0, ri = 0.6). Convergent in *Diapoma obi*, *Hemibrycon surinamensis* nodes 415, 416 and 420.
4. Anterior margin of basihyal (205: 0 > 1): margin expanded, its width two-thirds or more of basihyal length (s = 11, ci = 0.1, ri = 0.4). Reversed in *Chrysobrycon guahibo*, nodes 408, 409 and 411. Convergent in *Aulixidens eugeniae*, *Bryconamericus exodon* Eigenmann, *Diapoma speculiferum*, *Gephyrocharax major*, *G. torresi*, *Mimagoniates inequalis*, *Planaltina glandipedis*, and nodes 375 and 411.
5. Anterior tip of cleithrum (284: 0 > 1): reaching posterior margin of metapterygoid (Fig. 5A: s = 12, ci = 0.1, ri = 0.6). Reversed in *Gephyrocharax caucanus*, *G. sinuensis*, *Mimagoniates inequalis*, *Pterobrycon landoni*, and node 418. Convergent in *Bryconamericus mennii* Miquelarena, Protogino, Filiberto & López, *Carlastyanax aurocaudatus*, *Diapoma alburnus*, *D. speculiferum*, *Eretmobrycon scleroparius* (Regan), *Hemibrycon dariensis* Meek & Hildebrand, *Knodus breviceps*, *K. heteresthes* (Eigenmann), *Piabarchus analis* (Eigenmann), *Planaltina glandipedis*, and nodes 403 and 404.
6. Size of second postcleithrum relative to cleithrum (302: 0 > 1): postcleithrum small, almost completely covered by cleithrum (Fig. 3: states 0 and 1; s = 5, ci = 0.2, ri = 0.8). Convergent in *Scopaeocharax rhinodus*, and nodes 417 and 419.
7. Location of anterior pelvic bone tip (314: 1 > 0): tip anterior to rib of sixth vertebra (Fig. 5B: s = 20, ci = 0.1, ri = 0.5). Reversed in *Chrysobrycon guahibo*, *Eretmobrycon scleroparius*, *Gephyrocharax caucanus*, *G. chocoensis*, *G. martae*, *G. major*, *G. torresi*, *G. valencia*, *G. venezuelae*, and node 362. Convergent in *Bryconamericus yokiae*, *Carlastyanax aurocaudatus*, *Piabina thomasi* (Fowler), nodes 416 and 419.
8. Length of middle dorsal-fin rays (329: 0 > 1): middle rays longer than anterior and posterior rays (s = 8, ci = 0.1, ri = 0.7). Convergent in *Knodus tanaothoros* (Weitzman, Menezes, Evers & Burns) and nodes 417 and 420.

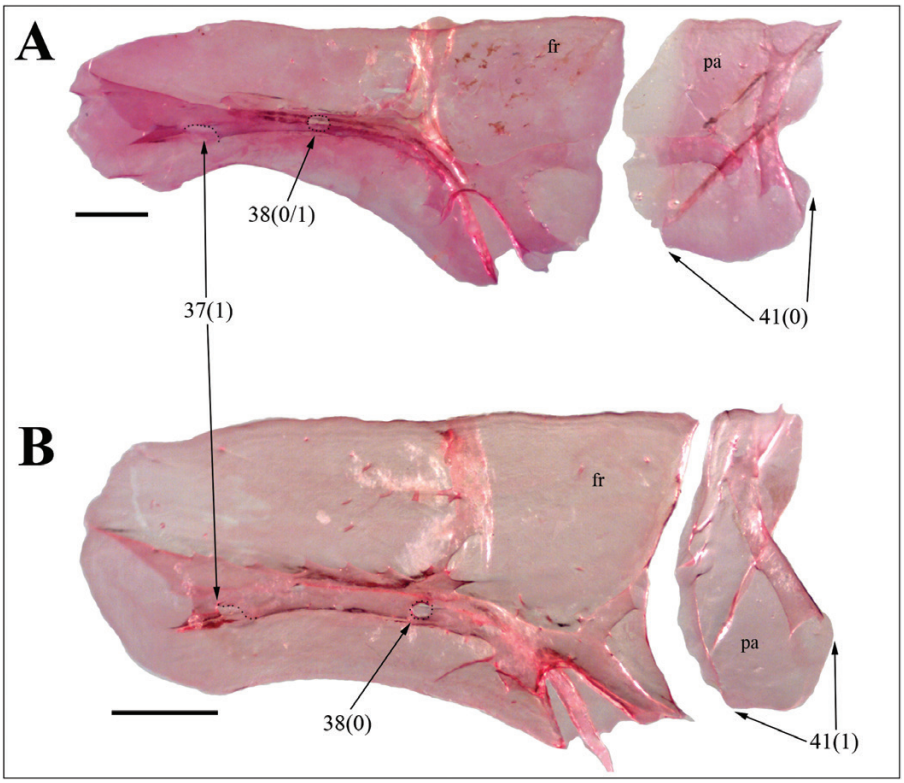

Figure 4. Frontal and parietal bones of *Bryconamericus* cf. *iheringii* (A), female, 62.4 mm SL, CI-FML 6107, and *Gephyrocharax intermedius* (B), female, 35.6 mm SL, CI-FML 6107. Arrows indicate characters analyzed in the data matrix. Abbreviations in Table 1. Left dorsal view. Anterior to left. Scale bar: 1 mm.

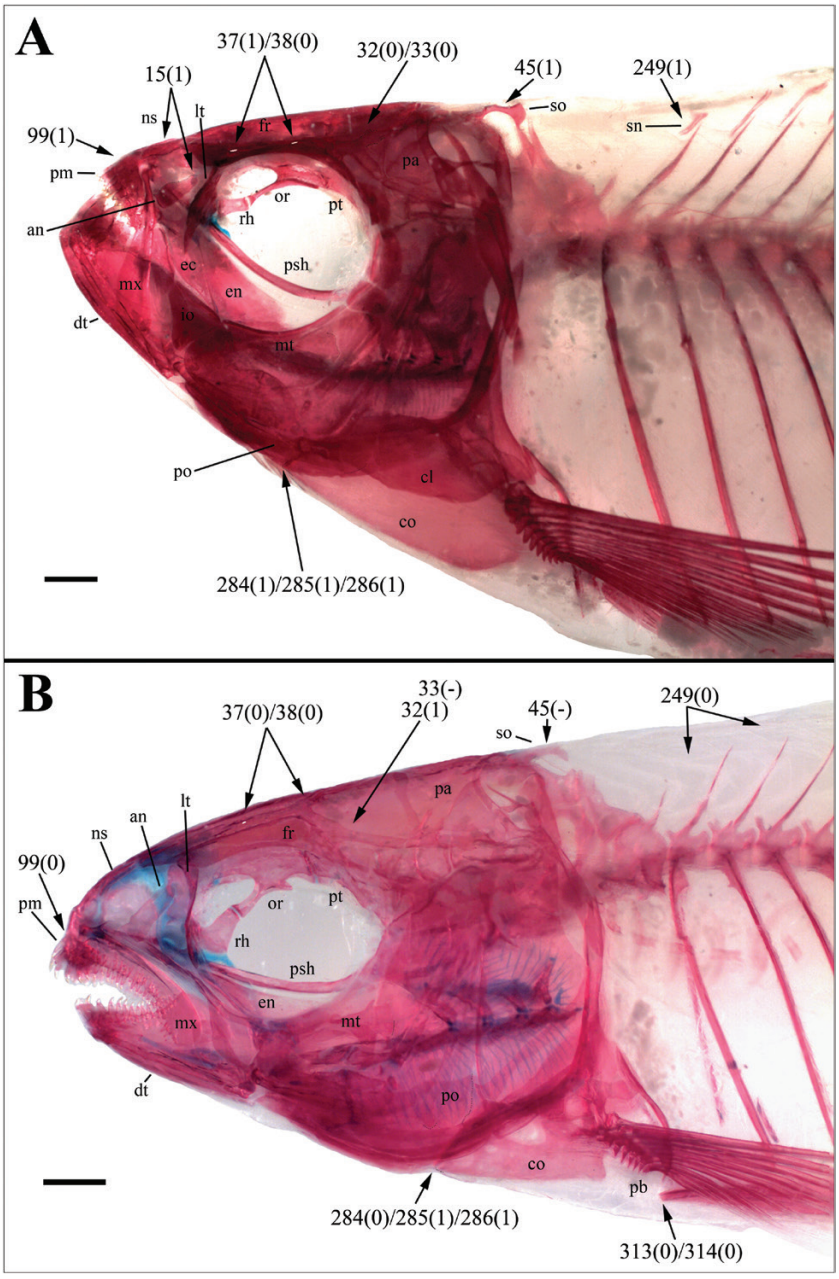

Figure 5. Skull and anterior region of body of *Gephyrocharax chocoensis* (A), male, 38.9 mm SL, IMCN 4830, and *Scopaeocharax rhinodus* (B), male, 25.7 mm SL, MUSM 8441. Arrows indicate characters analyzed in the data matrix. Abbreviations in Table 1. Left lateral view. Scale bar: 1 mm.

9. Proximal and medial radials of anal fin (335: 0 > 1): fused in most pterygiophores (s = 16, ci = 0.1, ri = 0.6). Reversed in *Chrysobrycon eliasi*, *Chrysobrycon guahibo*, *Corynopoma riisei*, *Gephyrocharax caucanus*, *G. chocoensis*, *G. major*, and node 412. Convergent in *Scopaeocharax rhinodus*, *Tyttocharax* sp. and *Xenurobrycon macropus*.
10. Grooves with neuromasts in head above eyes (406: 0 > 1): present, well developed (s = 2, ci = 0.5, ri = 1). Convergent in node 417.

Node 401 (100/100/93/55) Chrysobrycon

1. Frontal fontanel (26: 0 > 1): absent (s = 9, ci = 0.1, ri = 0.5). Reversed in *G. intermedius*. Convergent in

Gephyrocharax martae, *G. torresi*, *Pterobrycon myrnae*, and node 406.

2. Parietal fontanel in adults (40: 0 > 1): absent or reduced (s = 8, ci = 0.1, ri = 0.5). Convergent in *Gephyrocharax chocoensis*, *G. major*, *Pterobrycon myrnae*, and node 418.
3. Height of dorsolateral process of anguloarticular (130: 0 > 1): greatest vertical dimension of dorsolateral process as large as that of posterior region of horizontal process of anguloarticular (s = 3, ci = 0.3, ri = 0.8). Reversed in *Chrysobrycon guahibo* (Fig. 6: state 0). Convergent in *Acrobrycon ipanquianus*, *Gephyrocharax chocoensis*, and nodes 403, 386 and 385.
4. Length of posterior margin of hypural 2 (347: 0 > 1): posterior margin as large as vertical distance between bases of caudal-fin rays 11–13 (Fig. 7B: s = 18, ci = 0.1, ri = 0.3). Reversed in *Bryconamericus yokiae*, *Creagrutus anary* and *Piabina argentea*. Convergent in *Acrobrycon ipanquianus*, *Argopleura magdalenensis* (Eigenmann), *Attonitus ephimeros* Vari & Ortega, *Bryconamericus rubropictus*, *Eretmobrycon scleroparius*, *Gephyrocharax intermedius*, *G. major*

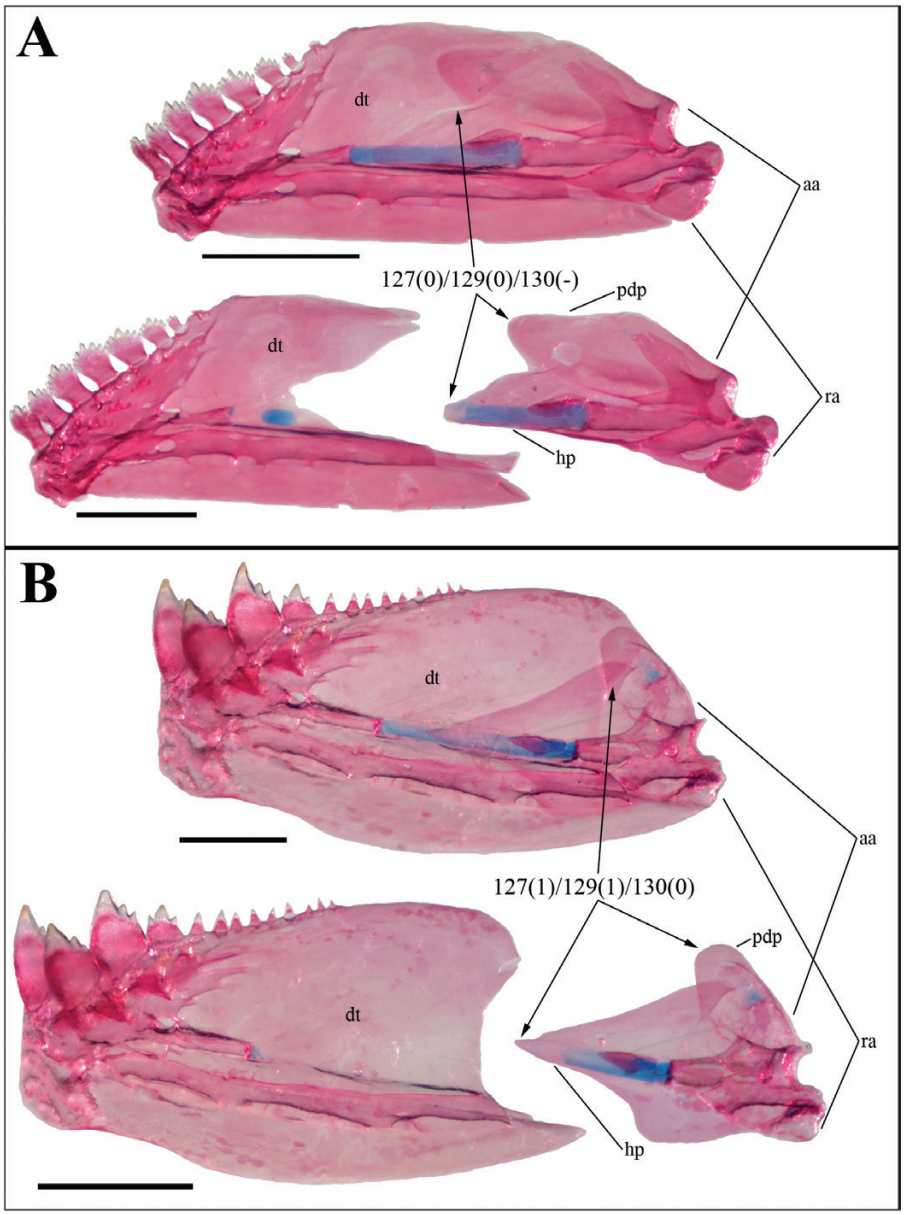

Figure 6. Lower jaw of *Odontostilbe pulchra* (A), female, 33.9 mm SL, MBUCV 33839, and *Pterobrycon myrnae* (B), female, 29.2 mm SL, ANSP 164243. Arrows indicate characters analyzed in the data matrix. Abbreviations in Table 1. Left lateral view. Scale bar: 1 mm.

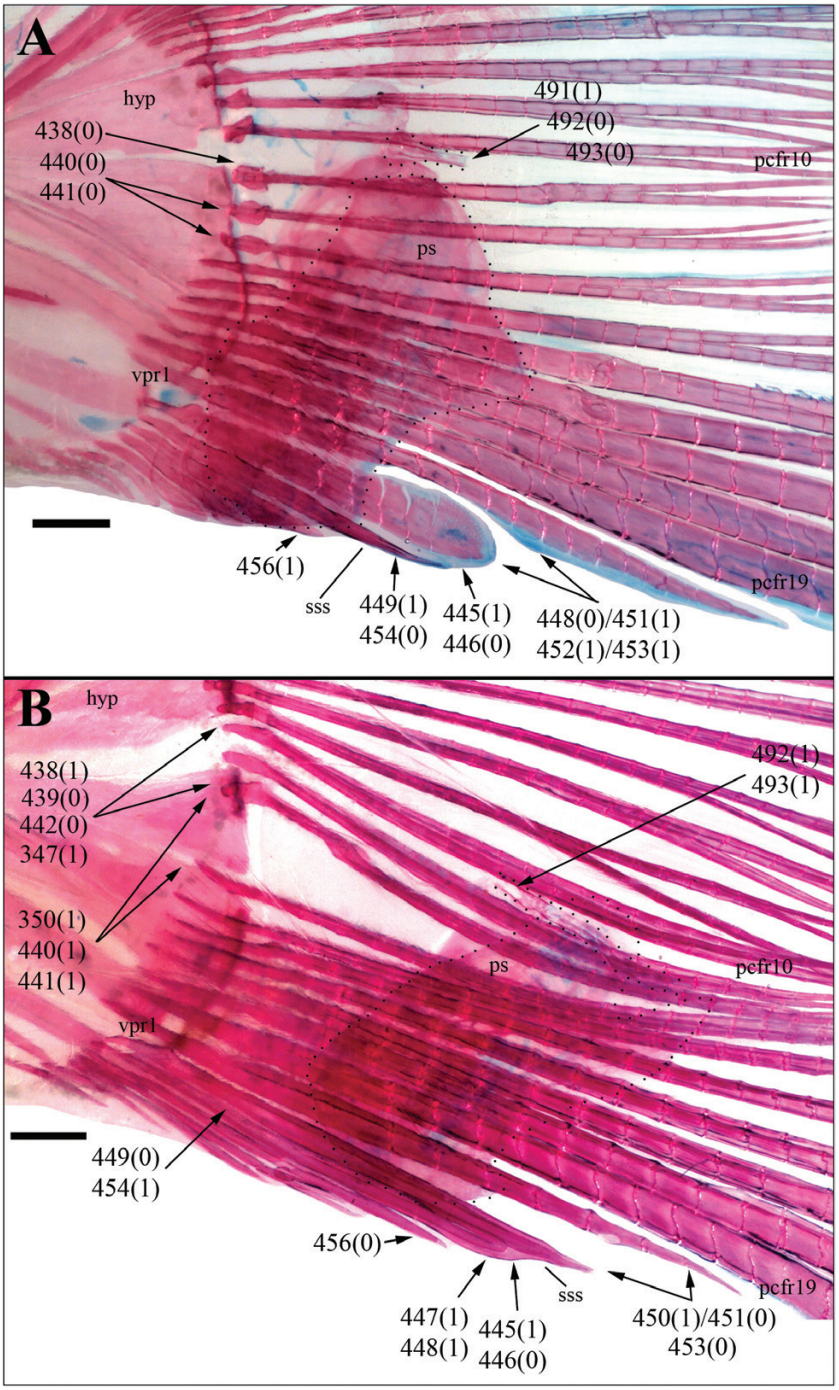

Figure 7. Detail of the lower caudal-fin skeleton of *Gephyrocharax intermedius* (A), male, 42.6 mm SL, STRI 1209, and *G. major* (B), male, 49.4 mm SL, MUSM 8518. Arrows indicate characters analyzed in the data matrix. Abbreviations in Table 1. Left lateral view. Scale bar: 1 mm.

Planaltina glandipedis, *Pseudocorynopoma doriae* Perugia, and nodes 381 and 384.

5. Terminal position of *interradialis* muscles relative to pouch scale in adult males (483: 1 > 0): fibres not exceeding posterodorsal border of such scale (s = 3, ci = 0.3, ri = 0.8). Reversed in node 414 (Fig. 8). Convergent in node 408.
6. Pouch-scale form in adult males (502: 0 > 1): pouch scale horizontally folded, forming laterally concave pocket (s = 1, ci = 1, ri = 1).

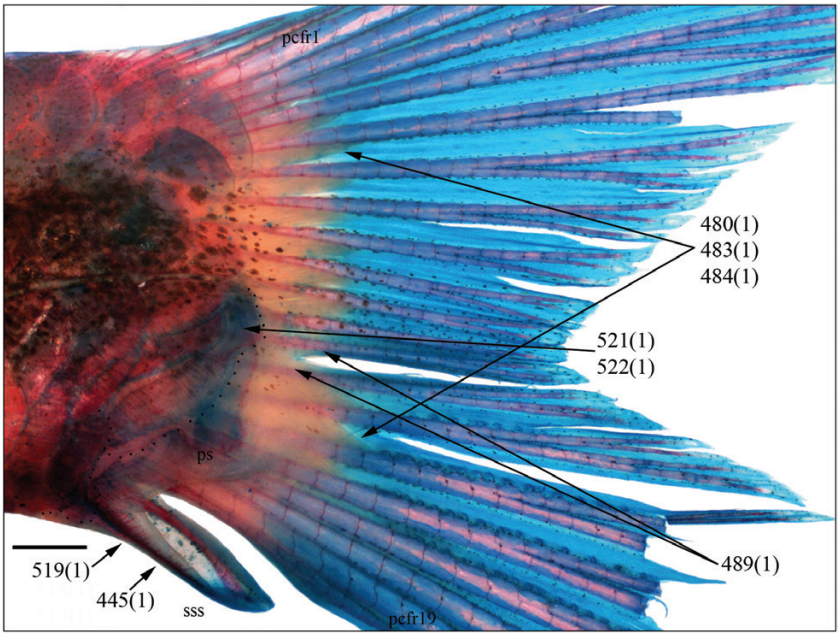

Figure 8. Caudal fin of *Gephyrocharax melanocheir*, male (A), 32.8 mm SL, CAR 73. Arrows indicate characters analyzed in the data matrix. Black dots delimit scales overlapping pouch scale. Abbreviations in Table 1. Left lateral view. Scale bar: 1 mm.

7. Number of pouch-scale *radii* in adult males (507: 1 > 0): 35 or fewer (Fig. 9A: s = 6, ci = 0.2, ri = 0.6). Reversed in *Gephyrocharax melanocheir*. Convergent in *Corynopoma riisei*, *G. sinuensis*, *G. venezuelae*, and nodes 405, 411 and 413.
8. Medial accessory pouch scale in adult males (525: 0 > 1): present (s = 1, ci = 1, ri = 1).

Node 418 (100/100/98/100) Pterobrycon

1. Location of anterior pelvic bone tip (313: 1 > 0): tip anterior to rib of fifth vertebra (Fig. 5B: s = 5, ci = 0.2, ri = 0.3). Convergent in *Chrysobrycon yoliae*, *Mimagoniates inequalis*, *Tyttocharax* sp., and node 419.
2. Number of rays on posteriormost anal-fin pterygiophore (337: 0 > 1): 1 (s = 5, ci = 0.2, ri = 0.2). Convergent in *Diapoma pyrrhopteryx* and *Tyttocharax* sp.
3. Size of pelvic-fin rays in adult males (422: 0 > 1): middle, especially fifth to seventh rays longer than remaining rays (s = 1, ci = 1, ri = 1).
4. Flank scales located near humeral region of body in adult males (494: 0 >1): one or two modified, paddle-shaped scales (s = 1, ci = 1, ri = 1).

Node 394 (100/100/38/16) Corynopoma + Gephyrocharax

1. Second, third and occasionally fourth ventral procurrent caudal-fin rays in adult males (445: 0 > 1): curved, and flattened, with similar length, and forming one or two spur-shaped structures (Figs 7–9A: s = 1, ci = 1, ri = 1).
2. Ventral margin of first ventral procurrent ray in adult males (451: 0 > 1): margin concave on middle portion of ray (Fig. 7: states 0 and 1; s = 2, ci = 0.5, ri = 0.7). Reversed in *Gephyrocharax major*.
3. Pouch-scale size in adult males (513: 0 > 1): pouch scale very large, its greatest vertical dimension equal or greater than half distance between hypural fan and distal tips of middle caudal-fin rays (Fig. 9A: s = 2, ci = 0.5, ri = 0.9). Convergent in node 419.
4. Spermatozeugmata (532: 0 > 1): present (s = 3, ci = 0.3, ri = 0.7). Reversed in node 351. Convergent in node 357.

Node 409 (100/100/31/16) Gephyrocharax

1. Development of *interradialis* between caudal-fin rays 12 and 13 in adult males (489: 0 > 1): *interradialis* muscles greatly developed posteroventrally, resulting in strong separation between rays (Fig. 8: s = 2, ci = 0.5, ri = 0.9). Reversed in *Gephyrocharax chocoensis* and *G. major* (Fig. 10). Convergent in *Landonia latidens*, *Pterobrycon landoni* and *P. myrnae*.
2. Number of terminal vertically arranged scales overlapping pouch scale in adult males (522: 0 > 1): 4 or 6 (Fig. 8: s = 4, ci = 0.3, ri = 0.7).

Node 408 (52/4/–15/16) Gephyrocharax atracaudatus + G. caucanus + G. chocoensis

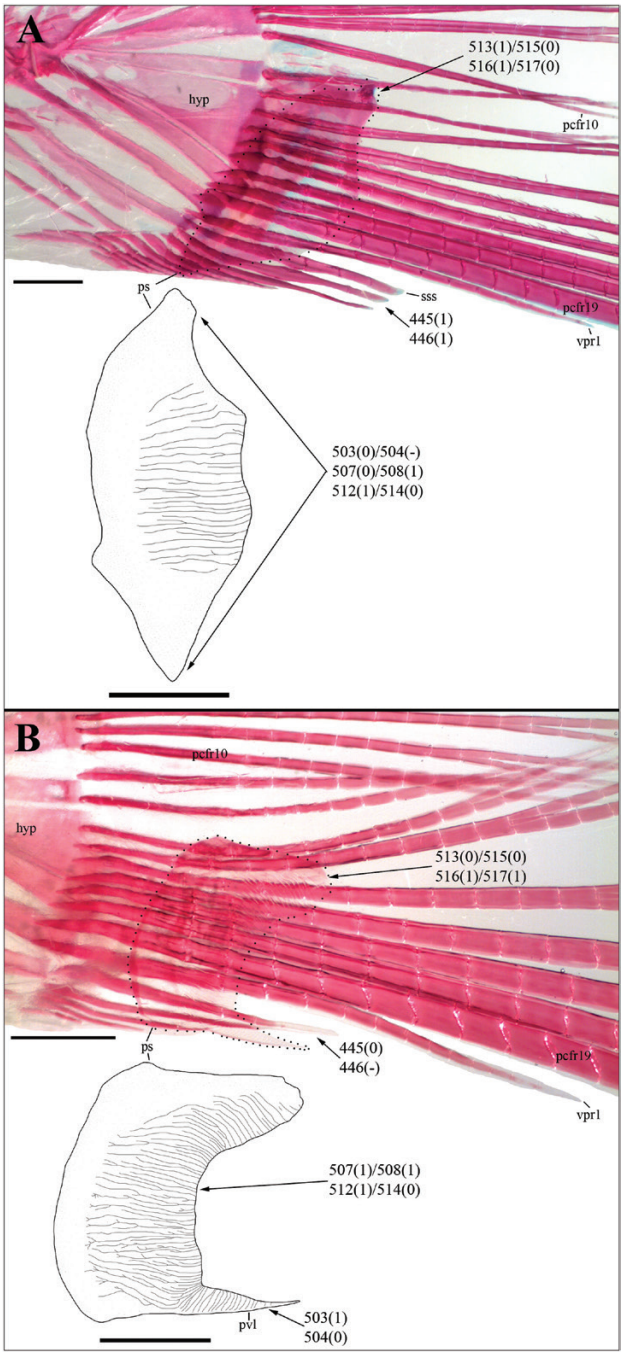

Figure 9. Detail of lower caudal-fin skeleton of *Corynopoma riisei* (A), male, 34.1 mm SL, MBUCV 285, and *Pterobrycon myrnae* (B), paratype male, 30.6 mm SL, LACM 338.001. Arrows indicate characters analyzed in the data matrix. Abbreviations in Table 1. Left lateral view. Scale bar: 1 mm.

+ G. intermedius + G. major + G. melanocheir + G. sinuensis + G. torresi + G. valencia + G. venezuelae

1. Humeral spot (394: 0 > 1): present (s = 2, ci = 0.5, ri = 0.8). Reversed in *Gephyrocharax caucanus*, *G. chocoensis*, *G. valencia*, *Knodus tanaothoros*, *Planaltina glandipedis*, and nodes 364, 396 and 415. Convergent in nodes 408 and 414.
2. Length of third ventral procurrent ray in adult males (454: 0 > 1): ray reaching or exceeding midpoint of first ventral procurrent ray (s = 9, ci = 0.1, ri = 0.5). Reversed in *Gephyrocharax valencia* and node 405. Convergent in *Acrobrycon ipanquianus*, *Bryconamericus* cf. *iheringii* (Boulenger), *B. rubropictus*, *Diapoma obi*, *Planaltina glandipedis*, *Pseudocorynopoma doriae*, and node 400.
3. Posterior extent of *interradialis* bundles on upper caudal-fin lobe in adult males (481: 1 > 0): most *interradialis* bundles not distinctively developed or lengthened posteriorly (Fig. 10: s = 3, ci = 0.3, ri = 0.8). Reversed in *Gephyrocharax atracaudatus*. Convergent in *Pseudocorynopoma doriae*.
4. Posterior extent of *interradialis* bundles on lower caudal-fin lobe in adult males (482: 0 > 1): *interradialis* bundles, especially those located between caudal rays 11 and 14, extending slightly more posteriorly than *interradialis* bundles located on dorsal lobe (Fig. 10: s = 3, ci = 0.3, ri = 0.8). Reversed in *Gephyrocharax chocoensis* and *G. atracaudatus*. Convergent in *Pseudocorynopoma doriae*.
5. Terminal position of *interradialis* muscles relative to pouch scale in adult males (483: 1 > 0): *interradialis* fibres not exceeding posterodorsal border of this scale (s = 3, ci = 0.3, ri = 0.8). Reversed in node 414 (Fig. 8). Convergent in node 401.

Node 407 (33/–14/–40/23) Gephyrocharax atracaudatus + G. chocoensis + G. intermedius + G. major

1. Posterior extent of pouch scale in adult males (515: 0 > 1): pouch scale extending beyond vertical crossing distal tip of second ventral procurrent ray (s = 5, ci = 0.2, ri = 0.4). Reversed in *Argopleura magdalenensis*, *Gephyrocharax major*, and node 396 (Fig. 9). Convergent in *G. caucanus*, *G. sinuensis*, *G. martae*, *Pterobrycon landoni*, and nodes 401 and 419.

Node 406 (52/4/–18/30) Gephyrocharax atracaudatus + G. intermedius + G. major

1. Frontal fontanel (26: 0 > 1): absent (s = 9, ci = 0.1, ri = 0.5). Reversed in *Gephyrocharax intermedius*. Convergent in *G. martae*, *G. torresi*, *Pterobrycon myrnae*, and node 401.
2. Types of spur-shaped structures in adult males (447: 0 > 1): second and third ventral procurrent rays straight or slightly curved along their lengths (Figs 7B, 9A: s = 1, ci = 1, ri = 1).

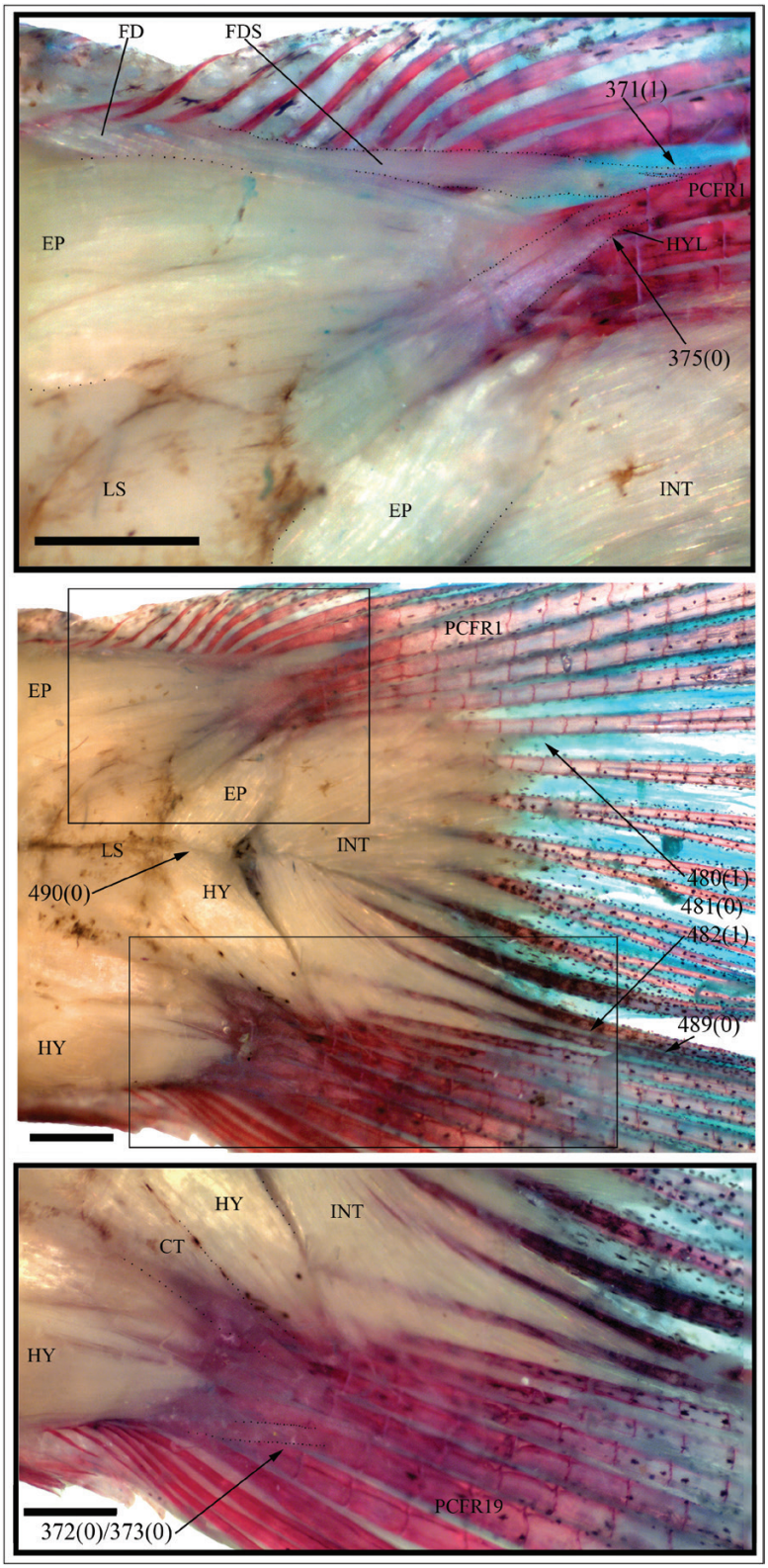

Figure 10. Most caudal-fin muscles of *Gephyrocharax major*, male, 44.9 mm SL, UMSS 5289. At the top, some fibre bundles of *epaxialis* and *interradialis* were removed. Scales and skin were removed. Abbreviations in Table 1. Left lateral view. Scale bar: 1 mm.

3. Posterior lobes on posterior border of pouch scale in adult males (503: 1 > 0): absent or reduced (Fig. 9A: s = 4, ci = 0.3, ri = 0.7). Reversed in *Pseudocorynopoma doriae*, *Pterobrycon myrnae*, *Xenurobrycon macropus*, and nodes 396 and 409 (Fig. 9B). Convergent in *Corynopoma riisei* and *Pterobrycon landoni*.

Node 405 (100/100/93/100) Gephyrocharax atracaudatus + G. intermedius

1. *Hemiradii* of posterior portion of third ventral procurrent ray in adult males (449: 0 > 1): strongly expanding laterally, especially on anterior portion (Fig. 7: states 0 and 1; s = 1, ci = 1, ri = 1).
2. Morphology of first and second ventral procurrent rays in adult males (452: 0 > 1): rays well associated spatially, ventral margin of middle region of first procurrent ray greatly concave and posterodorsal margin of second procurrent ray extremely expanded sagittally (s = 1, ci = 1, ri = 1).
3. Length of second ventral procurrent ray in adult males (453: 0 > 1): ray shorter or equal to half-length of first ventral procurrent ray (Fig. 7: states 0 and 1; s = 1, ci = 1, ri = 1).
4. Length of third ventral procurrent ray in adult males (454: 1 > 0): ray not reaching midpoint of first ventral procurrent ray (Fig. 7A: s = 9, ci = 0.1, ri = 0.5). Reversed in *Acrobrycon ipanquianus*, *Axelrodia lindeae* Géry, *Bryconamericus* cf. *iheringii*, *B. rubropictus*, *Diapoma obi*, *Pseudocorynopoma doriae*, and nodes 400 and 408.
5. Distal portion of fourth ventral procurrent ray in adult males (456: 0 > 1): portion flattened sagittally and slightly curved (Fig. 7: states 0 and 1; s = 3, ci = 0.3, ri = 0.7). Convergent in *Axelrodia lindeae*, *Gephyrocharax martae*, and node 412.
6. Number of pouch-scale *radii* in adult males (507: 1 > 0): 35 or fewer (Fig. 9A: s = 6, ci = 0.2, ri = 0.6). Reversed in *Gephyrocharax melanocheir*, *G. sinuensis* and *G. venezuelae*. Convergent in nodes 401, 411 and 413.

Node 413 (42/4/–27/23) Gephyrocharax caucanus + G. melanocheir + G. sinuensis + G. torresi + G. valencia + G. venezuelae

1. Synchondral articulation between lateral ethmoid and anterodorsal border of orbitosphenoid (23: 1 > 0): present (s = 9, ci = 0.1, ri = 0.7). Reversed in node 410. Convergent in *Bryconamericus rubropictus*, *Chrysobrycon guahibo*, *Knodus pectinatus*, and nodes 390 and 416.
2. Horizontal process of anguloarticular (127: 1 > 0): laterally covered by dentary only anteriorly (Fig. 6: s = 15, ci = 0.1, ri = 0.8). Reversed in *Hemibrycon plutarcoi* Román-Valencia and nodes 359, 395, 397, 401 and 420. Convergent in *Aulixidens eugeniae*, *Bryconamericus mennii*, *B. indefessus*, *Gephyrocharax chocoensis*, *G. intermedius*, *Pseudocorynopoma doriae*, nodes 354, 365 and 367.

Node 412 (33/–4/–7/43) Gephyrocharax caucanus + G. melanocheir + G. sinuensis + G. torresi + G. valencia

1. Urogenital papilla in adult females (408: 0 > 1): inconspicuous, not projecting externally to urogenital pore (s = 2, ci = 0.5, ri = 0.8).
2. Distal portion of fourth ventral procurrent ray in adult males (456: 0 > 1): flattened sagittally and slightly curved (s = 3, ci = 0.3, ri = 0.7). Convergent in *Axelrodia lindeae*, *Gephyrocharax martae*, and node 405.

Node 411 (52/14/–10/29) Gephyrocharax caucanus + G. melanocheir + G. torresi + G. valencia

1. Connective tissue extending over dorsal portion of pouch scale in adult males (506: 0 > 1): tissue attaching pouch scale to point between caudal-fin rays 15 and 17 (s = 1, ci = 1, ri = 1). Reversed in *Corynopoma riisei*, *Gephyrocharax venezuelae*, and nodes 401, 405 and 413. Convergent in *G. melanocheir* and *G. sinuensis*.

Node 410 (52/14/3/50) Gephyrocharax caucanus + G. melanocheir + G. torresi

1. Synchondral articulation between lateral ethmoid and anterodorsal border of orbitosphenoid (23: 0 > 1): absent, with orbitosphenoid distant from lateral ethmoid (s = 9, ci = 0.1, ri = 0.7). Reversed in *Bryconamericus rubropictus*, *Chrysobrycon guahibo*, *Knodus pectinatus*, and nodes 390, 413 and 416.
2. Form of external urogenital papilla form in adult females (409: 1 > 0): triangular, partially oriented posteroventrally (s = 1, ci = 1, ri = 1).

Node 414 (100/100/87/55) Gephyrocharax melanocheir + *G. torresi*

1. Outermost branched pectoral-fin in adult males (419: 0 > 1): with its distal branches forming fan-shaped structure (s = 1, ci = 1, ri = 1).
2. Pectoral-fin bony hooks in adult males (461: 0 > 1): present (s = 10, ci = 0.1, ri = 0.4). Convergent in

Bryconamericus cf. *iheringii*, *B. rubropictus*, and nodes 380 and 404.

3. Bony hooks on outermost pelvic-fin ray in adult males (466: 0 > 1): present (s = 14, ci = 0.1, ri = 0.4). Reversed in *Gephyrocharax major*. Convergent in *Aulixidens eugeniae*, *Bryconamericus indefessus*, *B. lethostigmus*, *B.* cf. *iheringii*, *Diapoma pyrrhopteryx*, *G. atracaudatus*, *G. chocoensis*, *Xenurobrycon macropus*, and nodes 400, 407 and 416.
4. Terminal position of *interradialis* muscles relative to pouch scale in adult males (483: 0 > 1): fibres surpassing posterodorsal border of this scale (Fig. 8: s = 3, ci = 0.3, ri = 0.8). Reversed in nodes 401 and 408.
5. Distal portion of outermost branched pectoral-fin ray (526: 0 > 1): pigmented, chromatophores forming dark spot, sometimes diffuse (s = 3, ci = 0.3, ri = 0.3). Convergent in *Gephyrocharax martae* and *Pseudocorynopoma doriae*.

DISCUSSION

MONOPHYLY AND INTERSPECIFIC RELATIONSHIPS OF *GEPHYROCHARAX*

The results obtained support the monophyly of *Gephyrocharax*, as currently defined taxonomically by Vanegas-Ríos (2016), and constitute the first phylogenetic hypothesis of all its species. However, in the present study, the presence of a spur-shaped structure formed by the second and third ventral procurrent rays in adult males, which is considered as the main diagnostic characteristic of *Gephyrocharax* (Vanegas-Ríos, 2016), was not recovered as a synapomorphy for the genus. Comparatively, *Corynopoma* has two spur-shaped structures formed by the second and third ventral procurrent rays and the third and fourth ventral procurrent rays. The spur-shaped structures are coded in the data matrix as an additive series divided into two characters: presence/absence and the number of the spur-shaped structures. The presence of spurs is a synapomorphy for the clade formed by *Corynopoma* + *Gephyrocharax*, but the presence of one spur (vs. two) was not obtained for the *Gephyrocharax* clade. This result was independent of the coding strategy used; when the character was coded in either an ordered or unordered multistate series, the same conclusion was reached.

Character 489, which resulted in one of the two synapomorphies supporting the *Gephyrocharax* clade, had some reversals and convergences with other stevardiines. This character describes the development of the *interradialis* fibres that are located between caudal-fin rays 12 and 13 in adult males. Most *Gephyrocharax* species have these fibres greatly developed posteroventrally in adult males, resulting in a strong separation between caudal-fin rays 12 and 13 (state 1). In *G. chocoensis, L. latidens*, *P. landoni* and *P. myrnae*, character 489 was coded as polymorphic because of the lack of appropriate specimens or the observation of an intermediate condition (additional details in Supporting Information, Appendix S3). As result, the synapomorphy was not optimised without homoplasy on the final topology. Additionally, character 489 was coded with state 0 in *G. major* (i.e. the *interradialis* fibres are little developed posteroventrally, resulting in a moderate separation between caudal-fin rays 12 and 13), which consequently constitutes a reversal within the genus. Despite these homoplastic variations, all *Gephyrocharax* species were assigned to the same node because they shared other synapomorphies, supporting clades that are more inclusive.

Corynopoma and *Gephyrocharax* were found as sister genera. Conversely, Weitzman & Menezes (1998) proposed that *Corynopoma* and *Pterobrycon* were sister genera based on a single synapomorphy (character 46, herein numbered 428 in Supporting Information, Appendix S3): the presence in adult males of '…an expansive anal-fin size in terms of the long length of the fin rays…'. In comparison with the phylogenetic study of Weitzman & Menezes (1998), the *Corynopoma* plus *Gephyrocharax* clade was recovered based on four synapomorphies related to sexual dimorphism of adult males (characters 445, 451, 513 and 532). Weitzman & Menezes (1998) used 40 sexually dimorphic characters and 11 non-dimorphic characters, most of which are associated with caudal-fin morphology of adult males. The phylogenetic significance of the characters of Weitzman & Menezes (1998) was re-evaluated in the present cladistic analysis, which resulted in a different scheme of phylogenetic relationships for *Gephyrocharax* [(node 395, (*Pterobrycon* (*Corynopoma*, *Gephyrocharax*)) vs. (*Gephyrocharax* (*Corynopoma*, *Pterobrycon*))]. Most of the morphological evidence used by Weitzman & Menezes (1998) was further reanalysed by Ferreira *et al.* (2011) as part of a phylogenetic study of most stevardiines (*sensu* Weitzman *et al.*, 2005), but *Corynopoma* and *Pterobrycon* were not included. Ferreira *et al.* (2011) recovered *Gephyrocharax* as the sister group of a clade comprising Xenurobryconini plus Hysteronotini (*sensu* Weitzman *et al.*, 2005). Here, *Gephyrocharax* and *Corynopoma* are recovered as sister genera in the final consensus topology, which agrees with the results of recent molecular studies that did not include *Pterobrycon* (Oliveira *et al.*, 2011; Thomaz *et al.*, 2015).

The majority of the interspecific relationships of *Gephyrocharax* species were defined by synapomorphies related to caudal-fin morphology of adult males. Based on the results obtained, two large clades (nodes

407 and 413) are hypothesised within *Gephyrocharax*: (1) *G. chocoensis* + (*G. major* + (*G. intermedius* + *G. atracaudatus*))) and (2) *G. venezuelae* + (*G. sinuensis* + (*G. valencia* + (*G. caucanus* + (*G. melanocheir* + *G. torresi*))))). The first clade (node 407) was supported by a single synapomorphy (character 515, state 1: pouch scale extends beyond a vertical through the distal tip of the second procurrent rays in adult males) that is reversed in *G. major* (state 0: pouch scale reaching but not extending beyond a vertical through the distal tip of the second procurrent rays in adult males), a species in which the character was coded as polymorphic. The second clade (node 413) is supported by two synapomorphies [state 0: characters 23 and 127), one of which is reversed in the node 410 [character 23, state 1: (*G. caucanus* + (*G. melanocheir* + *G. torresi*)]. Despite the large amount of morphological evidence analyzed in the data matrix, the number of synapomorphies (especially optimised without homoplasy) obtained for each clade within *Gephyrocharax* is relatively low (ranging from one to six). In fact, only two sister-group relationships found within *Gephyrocharax* were recovered with relatively high support values (>60 in GC values and rbs): *G. atracaudatus* + *G. intermedius* and *G. melanocheir* + *G. torresi*.

In the data matrix, three characters (526–528) associated with pigmentation of adult males were analyzed, but only one of these (526, state 1: the presence of dark pigmentation on the distal tip of outermost branched pectoral-fin ray in adult males) supported a clade within *Gephyrocharax* (node 414: *G. melanocheir* + *G. torresi*). The presence of a humeral spot (character 394: state 1) was obtained as a synapomorphy of node 408 (including most *Gephyrocharax* species except *G. martae*). However, this character was found moderately homoplastic (ci = 0.5, ri = 0.8) within Stevardiinae and *Gephyrocharax*, being reversed in *G. chocoensis*, *G. caucanus* and *G. valencia*. It seems that characters associated with body pigmentation can be informative at some phylogenetic level, as occurred here (e.g. humeral spot), but these can be as homoplastic as the diagnostic characteristics (e.g. lateral line) that Eigenmann (1917) used to define the intergeneric limits within the Characidae (Mirande, 2010).

Previous morphology-based studies of Glandulocaudinae or Stevardiinae (*sensu* Weitzman *et al.*, 2005) have investigated intergeneric relationships with other characids, but none of these have tested interspecific phylogenetic relationships (Weitzman & Fink, 1985; Weitzman & Menezes, 1998; Castro *et al.*, 2003; Ferreira *et al.*, 2011). In their phylogenetic studies of Characidae (Mirande, 2010) and Stevardiinae (Mirande *et al.*, 2013), Mirande (2010) and Mirande *et al.* (2013) did not include any *Gephyrocharax* species in their morphological data sets and did not code most of the morphological variation associated with sexually dimorphic features that had been previously used to support the phylogeny of the Glandulocaudinae and/or its tribes (Weitzman & Menezes, 1998; Menezes & Weitzman, 2009). However, the interspecific relationships of some *Gephyrocharax* have been partly resolved in two genetic-based studies (Bonilla-Rivero & López-Rojas, 2013; Thomaz *et al.*, 2015). As part of a phylogeographic study including three *Gephyrocharax* species, Bonilla-Rivero & López-Rojas (2013) found that *G. venezuelae* was more related to an unidentified species of *Gephyrocharax* than to *G. valencia*. In the results found here, conversely, *G. venezuelae* was resolved as the sister species of a clade formed by *G. caucanus*, *G. melanocheir*, *G. sinuensis*, *G. torresi* and *G. valencia*. Thomaz *et al.* (2015) analyzed five *Gephyrocharax* species and recovered a sister-group relationship between *G. atracaudatus* and *G. intermedius*, consistent with the phylogenetic hypothesis obtained here (Fig. 2). Additionally, Thomaz *et al.* (2015) found that *G. chocoensis* was the sister species of the clade consisting of *G. atracaudatus* plus *G. intermedius*. However, based on my results, *G. chocoensis* was resolved as the sister species of the clade formed by *G. major* + (*G. atracaudatus* + *G. intermedius*) (Fig. 2: node 406). During the preliminary searches using the IW method, the position of *G. martae* was found to be variable within the *Gephyrocharax* clade, often exchanged with *G. major*. However, despite this, the phylogenetic position of *G. martae* could be estimated based on the characters, only two of which were coded as missing entries for the species, that supported the different interspecific relationships within the genus.

In conclusion, the present study represents an advance of our understanding of the phylogeny of *Gephyrocharax* and Stevardiini. Both the IW and EW methods resolved the monophyly of the genus and the tribe (Fig. 2) and, additionally, several resulting clades of the IW consensus topology (Figs 1, 2) were congruent with those clades presented in the largest molecular phylogenetic study of Stevardiinae (Thomaz *et al.*, 2015).

Monophyly of *Chrysobrycon* and *Pterobrycon*

This is the first phylogenetic study proposing the monophyly of these genera, with *Chrysobrycon* being the sister group of the remaining stevardiins. The monophyly of *Chrysobrycon* was supported by eight synapomorphies, most of which are associated with caudal-fin squamation of adult males. The majority of these synapomorphies present reversals and/or convergences with other stevardiines, especially with genera that have a hypertrophied caudal-fin squamation

in the lower lobe of adult males (e.g. *Acrobrycon*, *Gephyrocharax* and *Pterobrycon*). The synapomorphies of *Chrysobrycon* involving the pouch scale of adult males (state 1 of the characters 502 and 525) were not observed in any other examined stevardiine. *Chrysobrycon mojicai* Vanegas-Ríos & Urbano-Bonilla (2017) was recently described from the Amazon Basin in Colombia. In that study, the presence of an extensive contact between the frontals (rarely the parietals) along the midline was identified as a diagnostic characteristic of the genus. Based on the results found here, this characteristic, which was coded in two characters (26 and 40), supports the monophyly of *Chrysobrycon*. The phylogenetic placement of *C. mojicai*, which could not be analyzed here, will be tested in a later study.

Thomaz *et al.* (2015) found that an unidentified species of *Gephyrocharax* was more related to *C. myersi* (the single species of *Chrysobrycon* included) than to the *Gephyrocharax* clade. In the results, conversely, both *Chrysobrycon* and *Gephyrocharax* were resolved as monophyletic groups in the consensus topologies, independent of the weighting scheme used (Fig. 2). Furthermore, the support measures obtained for the *Chrysobrycon* clade were relatively high (>50) in the final consensus topology. The findings of the taxonomic revision of *Gephyrocharax* (Vanegas-Ríos, 2016) suggest that the unidentified species of *Gephyrocharax* from the southwestern Amazon (Thomaz *et al.*, 2015) might correspond to *G. major*. Further examination of the specimens used by Thomaz *et al.* (2015) and molecular data for all *Chrysobrycon* species are needed to better understand the incongruences between both hypotheses. The two known species of *Pterobrycon* were resolved as a sister clade to *Corynopoma* and *Gephyrocharax*. This result differs from the traditional phylogenetic concept under which *Pterobrycon* and *Corynopoma* have been considered sister genera (Weitzman & Menezes, 1998). The *Pterobrycon* clade was supported by four synapomorphies related to anal and pelvic fins and body squamation of adult males. Additionally, only two of these synapomorphies were optimised without homoplasy on the most parsimonious trees used to calculate the final consensus topology (characters 422, state 1: the middle pelvic-fin rays are longer than the remaining rays; character 494, state 1: the presence of one or two paddle-shaped scales on the body in adult males). Even though the monophyly of *Pterobrycon* is not an unexpected result, it is indispensable for endorsing its current taxonomy (Bussing, 1974).

Comments on the monophyly and interrelationships of Stevardiini

Weitzman & Menezes (1998) carried out the first phylogenetic study that supported the monophyly of Stevardiini (=Corynopomini) consisting of the genera *Corynopoma*, *Gephyrocharax* and *Pterobrycon*. In subsequent morphology-based phylogenetic studies, including at least one stevardiin species, that definition of the tribe remained unchanged (Castro *et al.*, 2003; Weitzman *et al.*, 2005; Ferreira *et al.*, 2011). Mirande (2010) did not analyze any stevardiin species in his phylogenetic study of Characidae, but he tentatively assigned them to several nodes of his phylogenetic hypothesis (nodes 235–244 and 244) based on the placement of Stevardiini within the 'clade A' (*sensu* Malabarba & Weitzman, 2003) and the phylogenetic hypothesis of Glandulocaudinae (*sensu* Weitzman & Menezes, 1998). In my results, those nodes were not recovered with the same composition supposed by Mirande (2010) (Figs 1, 2).

Although *Hysteronotus megalostomus* Eigenmann and *Pseudocorynopoma heterandria* Eigenmann could not be coded in this work, the number of analyzed stevardiins is greater (20 species and 5 genera vs. 11 species and 4 genera) than that included in the most recent phylogenetic study of Stevardiinae (Thomaz *et al.*, 2015). The stevardiins are recovered as a monophyletic group in the final consensus topology [Fig. 2: (*Chrysobrycon* (*Pseudocorynopoma* (*Pterobrycon* (*Gephyrocharax*, *Corynopoma*))))]. Such congruence between morphological and molecular data reinforces the monophyly of the tribe as currently defined. The monotypic genus *Hysteronotus* is a putative member of Stevardiini (Thomaz *et al.*, 2015). Weitzman & Menezes (1998) and Ferreira *et al.* (2011) obtained a sister-group relationship between *Hysteronotus* and *Pseudocorynopoma*, a hypothesis also pointed out by Thomaz *et al.* (2015). In the results obtained here, Stevardiini was supported by ten synapomorphies, three of which can be observed in *H. megalostomus* (Menezes, Weitzman & Teixeira, 2016): the middle dorsal-fin rays are longer than the anterior and posterior dorsal-fin rays, the anterior tip of the premaxilla is horizontally aligned with the upper half of the orbit, and the presence of well-developed grooves with neuromasts along the dorsal surface of the head. Although none of the synapomorphies defining Stevardiini were optimised without homoplasy on the final phylogenetic hypothesis, the majority of these had relatively high values in the retention indices (ranging from 0.6 to 1).

In the final consensus, *Acrobrycon* was obtained as the sister group of Stevardiini, which disagrees with the traditional phylogenetic position of the genus as part of the Diapomini (Weitzman & Menezes, 1998; Arcila *et al.*, 2013). In a phylogenetic study using morphological, reproductive and spermatic characters, Ferreira *et al.* (2011) found *Acrobrycon* sister to a clade consisting of *Gephyrocharax* plus other xenurobryconin and hysterotonin genera (*sensu*

Weitzman & Menezes, 1998). However, more recently, *Acrobrycon* has been considered to be the sister group of *Hemibrycon* (Thomaz *et al.*, 2015).

Another stevardiine genus with a contentious position between the tribes allied to Stevardiini is *Argopleura*, which was obtained as the sister group of a clade including *Scopaeocharax*, *Tyttocharax* and *Xenurobrycon*. These genera have been grouped together in Xenurobryconini, a tribe related to the Stevardiini (Weitzman & Fink, 1985; Weitzman & Menezes, 1998). In the DNA-based phylogenetic study by Thomaz *et al.* (2015), *Argopleura* was resolved as the sister group of Glandulocaudini in most of their phylogenetic results, but in their ML tree it was obtained as the sister group of Glandulocaudini and Stevardiini. Based on these results, Thomaz *et al.* (2015) placed *Argopleura* as *incertae sedis* in Stevardiinae. The phylogenetic position obtained for *Argopleura* in the final consensus topology agrees more with that found by Weitzman & Fink (1985) and Weitzman & Menezes (1998) than with that found by Thomaz *et al.* (2015). Despite this disagreement between the molecular and morphological data, which should be investigated further, *Argopleura* is tentatively considered the sister genus of Xenurobryconini based on the results of the present study.

Comments on the interrelationships within Stevardiinae

Based on the type of cells constituting part of the glandular pocket (mucous vs. club), Weitzman *et al.* (2005) defined the stevardiines as a group consisting of the six tribes (Stevardiini = Corynopomini, Diapomini, Hysteronotini, Landonini, Phenacobryconini and Xenurobryconini) that had been previously placed in Glandulocaudinae by Weitzman & Menezes (1998). Later, Mirande (2010) expanded the phylogenetic concept of the subfamily to include the species of 'clade A' of Malabarba & Weitzman (2003). Since then, the monophyly of Stevardiinae has been widely supported based on molecular data (Javonillo *et al.*, 2010; Oliveira *et al.*, 2011; Thomaz *et al.*, 2015). In the final tree topology (Figs 1, 2), the monophyly of Stevardiinae was resolved with 26 of the 44 genera recognised in this subfamily by Mirande (2010), Mirande *et al.* (2013) and Thomaz *et al.* (2015). In total, 73 stevardiine species were analyzed in the data matrix, whereas Mirande (2010) and Mirande *et al.* (2013) analyzed 27 and 41 stevardiines, respectively (excluding *Creagrutus* species added in their extended matrix). After comparing the results with those presented by Mirande (2010) and Mirande *et al.* (2013), most of the differences found among the final topologies are associated with the placement of the species of *Bryconamericus*, *Diapoma* and *Knodus*, which in all cases did not constitute monophyletic groups. Additionally, the final tree topology (Fig. 1) recovered the monophyly of a group consisting of *Carlastyanax*, *Creagrutus* and *Piabina*, which was proposed by Mirande *et al.* (2013).

Markiana was obtained within the *Astyanax* Baird & Girard clade instead of the stevardiine clade (Supporting Information, Appendix S6), which disagrees with recent molecular phylogenetic studies that placed the genus within Stevardiinae (Oliveira *et al.*, 2011; Thomaz *et al.*, 2015). According to Baicere-Silva *et al.* (2011), the genus should be considered a putative member of Stevardiinae since the spermatozoa of its type species [*M. nigripinnis* (Perugia)] share the characteristics of the non-inseminating members of the subfamily.

In respect to other stevardiines, the *Eretmobrycon* species were found within the Stevardiinae clade, which is consistent with the phylogenetic result proposed by Thomaz *et al.* (2015). This finding was not obtained in previous morphology-based phylogenetic studies (Mirande, 2009; Mirande *et al.*, 2011; Mirande *et al.*, 2013). Other genera such as *Phenacobrycon* and *Landonia* were resolved as sister groups within the subfamily and, remarkably, they were not found to be closely related to the genera with which they have been traditionally placed in Glandulocaudinae (*sensu* Weitzman & Menezes, 1998), in the Stevardiinae (*sensu* Weitzman *et al.* 2005), or in the node 237 (similar to Glandulocaudinae in Weitzman & Menezes, 1998) by Mirande (2010).

Although the purpose of the present work may be considered as a reappraisal of the phylogenetic study of Stevardiinae by Mirande (2010) and Mirande *et al.* (2013), the primary object was the study of the phylogeny of *Gephyrocharax* and other stevardiins based on a large data matrix. The effect of adding Stevardiini (and other terminal taxa) to the data matrices of Mirande (2010) and Mirande *et al.* (2013) can be considered as a secondary result of the cladistic analysis presented herein, which represents an advance in the phylogenetic knowledge of the subfamily. It is evident that our understanding of the phylogenetic relationships of many stevardiines has improved in recent years (Malabarba & Weitzman, 2003; Mirande, 2010; Mirande *et al.*, 2013; Thomaz *et al.*, 2015), but further research is still needed to achieve a more consensual view of the internal classification of this subfamily.

ACKNOWLEDGEMENTS

I am indebted to María de las Mercedes Azpelicueta and Juan M. Mirande for advising and supporting me during the course of this work, which constitutes

part of my PhD thesis. The following individuals and institutions offered immeasurable help and assistance: Barbara Brown (AMNH); Mariangeles Arce, John Lundberg, Mark Sabaj-Perez and Kyle Luckenbill (ANSP); Jon Armbruster and David C. Werneke (AUM); Carlos Ardila-Rodríguez (CAR); Jon Fong and Dave Catania (CAS); Juan M. Mirande, Gastón Aguilera and Guillermo Terán (CI-FML); Luz Jiménez (CIUA); Jaider M. Peña, Francisco Villa-Navarro and Gladys Reinoso-Flórez (CZUT-IC); Mary Rogers, Leo Smith, Philip Willink, Susan Mochel, Kevin Swagel and Chris Jones (FMNH); José I. Mojica, Ofelia Mejía and Gustavo Ballen (ICNMHN); Armando Ortega, Gian C. Sánchez and Raúl Ríos (IMCN, INCIVA); Chris Taylor, Mike Retzer and Daniel Wylie (INHS); Christine Thacker, Molly Sjöberg and Katie Kramer (LACM); Francisco Provenzano (MBUCV); Carlos Lucena and Margarete Lucena (MCP); Karsten Hartel and Andrew Williston (MCZ); Ramiro Barriga (MEPN); Sonia Fisch-Muller (MHNG); María de las Mercedes Azpelicueta, Jorge Casciotta, Adriana Almirón, Amalia Miquelarena, Hugo López and Diego Nadalin (MLP); Hernán Ortega, Max Hidalgo, Giannina Trevejo, Junior Chuctaya, Lisveth Valenzuela and Vanessa Meza (MUSM); Lars Lundquist (MZLU); Bodil Kajrup and Sven O. Kullander (NRM); Stefan Koerber (Peces Criollos); Hernán López-Fernández (ROM); Phillip Willink (Shedd Aquarium); Ruth Reina (in memoriam) and Eldregde Bermingham (STRI); Larry Page and Rob Robins (UF); Mauricio Torres-Mejía and Martha Ramírez-Pinilla (UIST); Mabel Maldonado (UMSS); Richard Vari (in memoriam), Jeff Clayton, Lisa Palmer, Sandra Raredon and Dahiana Arcila (USNM); and Dawn Phillip and Mike Rutherford (UWIZM). I thank the CAS and FMNH for providing open access to a great volume of photographs and radiographs of the type material of characid species and to Ana Bonilla-Rivero (UCV), Donald Taphorn, Stanley Weitzman (USNM) and Naercio Menezes (MZUSP) for helping with useful information about *Gephyrocharax*. Guillermo Teran (CI-FML) helped with histological procedures. This research was supported by a Doctoral grant awarded by CONICET-Argentina (F. Villa-Navarro was co-advisor for the last time) and by the Fundación para la Promoción de la Investigación y la Tecnología, Banco de la República, Colombia (FPIT 2814). Additional financial supports were provided by the Facultad de Ciencias Naturales y Museo, UNLP (Expte: 1000-007351/2011), ANPCyT-PICT 913 (M. Azpelicueta), FONCyT-PICT 2011-0992 (J. Mirande) and the Smithsonian Institution (fellowship grant supervised by Richard Vari in memoriam). I am grateful to Luiz Fernandez (CONICET), Victor Cussac (CONICET) and Luiz Malabarba (UFRGS) for providing useful comments to a Spanish version of this paper and to Dawn Phillip and Donald Taphorn for improving the English writing. TNT is provided free by the Willi Hennig Society.

REFERENCES

Arcila D, Vari RP, Menezes NA. 2013. Revision of the Neotropical genus *Acrobrycon* (Ostariophysi: Characiformes: Characidae) with description of two new species. *Copeia* **2013:** 604–611.

Arias JS, Miranda-Esquivel DR. 2004. Profile parsimony (PP): an analysis under implied weights (IW). *Cladistics* **20:** 56–63.

Baicere-Silva CM, Ferreira KM, Malabarba LR, Benine RC, Quagio-Grassiotto I. 2011. Spermatic characteristics and sperm evolution on the subfamily Stevardiinae (Ostariophysi: Characiformes: Characidae). *Neotropical Ichthyology* **9:** 377–392.

Bonilla-Rivero A, López-Rojas H. 2013. On the origin and diversification of Venezuelan freshwater fishes: the genus *Gephyrocharax* (Ostariophysi: Characidae): a case study. *Neotropical Ichthyology* **11:** 487–496.

Bremer K. 1994. Branch support and tree stability. *Cladistics* **10:** 295–304.

Bussing WA. 1974. *Pterobrycon myrnae*, a remarkable new glandulocaudine characid fish from Costa Rica. *Revista de Biología Tropical* **22:** 135–159.

Castro RC, Ribeiro AC, Benine RC, Melo ALA. 2003. *Lophiobrycon weitzmani*, a new genus and species of glandulocaudine fish (Characiformes: Characidae) from the Rio Grande drainage, Alto Rio Paraná system, southeastern Brazil. *Neotropical Ichthyology* **1:** 11–19.

Datovo A, Bockmann FA. 2010. Dorsolateral head muscles of the catfish families Nematogenyidae and Trichomycteridae (Siluriformes: Loricarioidei): comparative anatomy and phylogenetic analysis. *Neotropical Ichthyology* **8:** 193–246.

Datovo A, Castro RM. 2012. Anatomy and evolution of the mandibular, hyopalatine, and opercular muscles in characiform fishes (Teleostei: Ostariophysi). *Zoology (Jena, Germany)* **115:** 84–116.

Datovo A, Vari RP. 2013. The jaw adductor muscle complex in teleostean fishes: evolution, homologies and revised nomenclature (Osteichthyes: Actinopterygii). *PLoS ONE* **8:** e60846.

Eigenmann CH. 1912. Some results from an ichthyological reconnaissance of Colombia, South America. Part I. *Indiana University Studies* **16:** 1–27.

Eigenmann CH. 1917. American Characidae [Part 1]. *Memoirs of the Museum of Comparative Zoology* **43:** 1–102.

Eigenmann CH, Myers GS. 1929. American Characidae [Part 5]. *Memoirs of the Museum of Comparative Zoology* **43:** 429–558.

Eschmeyer WN, Fong JD. 2017. Species by family/subfamily. Available at: http://researcharchive.calacademy.org/research/ichthyology/catalog/SpeciesByFamily.asp (accessed 17 February 2017).

Farris JS. 1970. Methods for computing Wagner trees. *Systematic Zoology* **19:** 83–92.

Farris JS. 1983. The logical basis of phylogenetic analysis. In: Platnick NI, Funk VA, eds. *Advances in Cladistics II*. New York: Columbia University Press, 7–36.

Farris JS. 1989. The retention index and the rescaled consistency index. *Cladistics* **5:** 417–419.

Ferreira KM, Menezes NA, Quagio-Grassioto I. 2011. A new genus and two new species of Stevardiinae (Characiformes: Characidae) with a hypothesis on their relationships based on morphological and histological data. *Neotropical Ichthyology* **9:** 281–298.

Fink SV, Fink WL. 1981. Interrelationships of the Ostariophysan fishes (Teleostei). *Zoological Journal of the Linnean Society* **72:** 297–353.

Fink WL, Weitzman SH. 1974. The so-called Cheirodontin fishes of Central America with descriptions of two new species (Pisces: Characidae). *Smithsonian Contributions to Zoology* **172:** 1–45.

Goloboff PA. 1993. Estimating character weights during tree search. *Cladistics* **9:** 83–91.

Goloboff PA. 1995. Parsimony and weighting: a reply to Turner and Zandee. *Cladistics* **11:** 91–104.

Goloboff PA. 1997. Self-weighted optimization: tree searches and character state reconstructions under implied transformation costs. *Cladistics* **13:** 225–245.

Goloboff PA. 1999. Analyzing large data sets in reasonable times: solutions for composite Optima. *Cladistics* **15:** 415–428.

Goloboff PA. 2014. Extended implied weighting. *Cladistics* **30:** 260–272.

Goloboff PA, Carpenter JM, Arias JS, Esquivel DRM. 2008a. Weighting against homoplasy improves phylogenetic analysis of morphological data sets. *Cladistics* **24:** 758–773.

Goloboff PA, Catalano SA. 2016. TNT version 1.5, including a full implementation of phylogenetic morphometrics. *Cladistics* **32:** 221–238.

Goloboff PA, Farris JS, Källersjö M, Oxelman B, Ramírez MJ, Szumik CA. 2003. Improvements to resampling measures of group support. *Cladistics* **19:** 324–332.

Goloboff PA, Farris JS, Nixon KC. 2008b. TNT, a free program for phylogenetic analysis. *Cladistics* **24:** 774–786.

Hennig W. 1966. *Phylogenetic systematics*. Urbana: University of Illinois.

Hoffmann M, Britz R. 2006. Ontogeny and homology of the neural complex of otophysan Ostariophysi. *Zoological Journal of the Linnean Society* **147:** 301–330.

Javonillo R, Malabarba LR, Weitzman SH, Burns JR. 2010. Relationships among major lineages of characid fishes (Teleostei: Ostariophysi: Characiformes), based on molecular sequence data. *Molecular Phylogenetics and Evolution* **54:** 498–511.

Lucena CA, Soares HG. 2016. Review of species of the *Astyanax bimaculatus* "caudal peduncle spot" subgroup *sensu* Garutti & Langeani (Characiformes, Characidae) from the rio La Plata and rio São Francisco drainages and coastal systems of southern Brazil and Uruguay. *Zootaxa* **4072:** 101–125.

Malabarba LR, Weitzman SH. 2003. Description of new genus with six new species from southern Brazil, Uruguay and Argentina, with a discussion of a putative characid clade (Teleostei: Characiformes: Characidae). *Comunicações do Museu de Ciências e Tecnologia da PUCRS, Série Zoologia* **16:** 67–151.

Mattox GM, Britz R, Toledo-Piza M. 2014. Skeletal development and ossification sequence of the characiform *Salminus brasiliensis* (Ostariophysi: Characidae). *Ichthyological Exploration of Freshwaters* **25:** 103–158.

Menezes NA, Weitzman SH. 2009. Systematics of the Neotropical fish subfamily Glandulocaudinae (Teleostei: Characiformes: Characidae). *Neotropical Ichthyology* **7:** 295–370.

Menezes NA, Weitzman SH, Teixeira TF. 2016. Redescription of *Hysteronotus megalostomus* (Characiformes: Characidae: Stevardiinae), a poorly known characid from tributaries of the Rio São Fancisco, Brazil with comments on the conservation of the species. *Journal of Fish Biology* **89:** 495–509.

Mirande JM. 2009. Weighted parsimony phylogeny of the family Characidae (Teleostei: Characiformes). *Cladistics* **25:** 574–613.

Mirande JM. 2010. Phylogeny of the family Characidae (Teleostei: Characiformes): from characters to taxonomy. *Neotropical Ichthyology* **8:** 385–568.

Mirande JM, Aguilera G, Azpelicueta MM. 2011. A threatened new species of *Oligosarcus* and its phylogenetic relationships, with comments on *Astyanacinus* (Teleostei: Characidae). *Zootaxa* **2994:** 1–20.

Mirande JM, Jerep FC, Vanegas-Ríos JA. 2013. Phylogenetic relationships of the enigmatic *Carlastyanax aurocaudatus* (Eigenmann) with remarks on the phylogeny of the Stevardiinae (Teleostei: Characidae). *Neotropical Ichthyology* **11:** 747–766.

Nelson GJ. 1969. Gill arches and the phylogeny of fishes with notes on the classification of the vertebrates. *Bulletin of the American Museum of Natural History* **141:** 475–522.

Oliveira C, Avelino GS, Abe KT, Mariguela TC, Benine RC, Ortí G, Vari RP, Corrêa e Castro RM. 2011. Phylogenetic relationships within the speciose family Characidae (Teleostei: Ostariophysi: Characiformes) based on multilocus analysis and extensive ingroup sampling. *BMC Evolutionary Biology* **11:** 275.

Patterson C. 1975. The braincase of pholidophorid and leptolepid fishes, with a review of the actinopterygian braincase. *Philosophical Transactions of the Royal Society of London, Series B: Biological Sciences* **269:** 275–579.

Roberts TR. 1973. The glandulocaudine characid fishes of the Guayas basin in western Ecuador. *Bulletin of the Museum of Comparative Zoology* **144:** 489–514.

Sabaj MH. 2016. Standard symbolic codes for institutional resource collections in herpetology and ichthyology: an online reference, Version 6.5. Available at: http://www.asih.org/resources/standard-symbolic-codes-institutional-resource-collections-herpetology-ichthyology (accessed 26 April 2016).

Schultz LP. 1944. The fishes of the family Characinidae from Venezuela, with descriptions of seventeen new forms. *Proceedings of the United States National Museum* **95:** 235–367.

Taylor WR, Dyke GCV. 1985. Revised procedures for staining and clearing small fishes and other vertebrates for bone and cartilage study. *Cybium* **9:** 107–119.

Terán GE, Mangione S, Mirande JM. 2014. Gill-derived glands in species of *Astyanax* (Teleostei: Characidae). *Acta Zoologica* **96:** 335–342.

Thomaz AT, Arcila D, Ortí G, Malabarba LR. 2015. Molecular phylogeny of the subfamily Stevardiinae Gill, 1858 (Characiformes: Characidae): classification and the evolution of reproductive traits. *BMC Evolutionary Biology* **15:** 146.

Vanegas-Ríos JA. 2014. *Revisión sistemática del género* Gephyrocharax *Eigenmann, 1912 (Characiformes: Characidae: Stevardiinae)*. Unpublished PhD thesis, Universidad Nacional de La Plata.

Vanegas-Ríos JA. 2016. Taxonomic review of the Neotropical genus *Gephyrocharax* Eigenmann, 1912 (Characiformes, Characidae, Stevardiinae). *Zootaxa* **4100:** 1–92.

Vanegas-Ríos JA, Azpelicueta MM, Mirande JM, Gonzales MDG. 2013. *Gephyrocharax torresi* (Characiformes: Characidae: Stevardiinae), a new species from the Río Cascajales basin, Río Magdalena system, Colombia. *Neotropical Ichthyology* **11:** 275–284.

Vanegas-Ríos JA, Urbano-Bonilla A. 2017. A new species of *Chrysobrycon* (Characiformes, Characidae, Stevardiinae) from the Amazon River basin in Colombia, with a new diagnostic characteristic for the genus. *Journal of Fish Biology* **90:** 2344–2362.

Weitzman SH. 1962. The osteology of *Brycon meeki*, a generalized characid fish, with an osteological definition of the family. *Stanford Ichthyological Bulletin* **8:** 1–77.

Weitzman SH. 2003. Subfamily Glandulocaudinae. In: Reis RE, Kullander SO, Ferraris Carl J. Jr., eds. *Check list of the freshwater fishes of South and Central America*. Porto Alegre: EDIPUCRS, 222–230.

Weitzman SH, Fink SV. 1985. Xenurobryconin phylogeny and putative pheromone pumps in Glandulocaudine fishes (Teleostei: Characidae). *Smithsonian Contributions to Zoology* **421:** 1–121.

Weitzman SH, Menezes NA. 1998. Relationships of the tribes and genera of Glandulocaudinae (Ostariophysi: Characiformes: Characidae) with a description of a new genus, *Chrysobrycon*. In: Malabarba LR, Reis RE, Vari RP, Lucena ZMSD, Lucena CA, eds. *Phylogeny and classification of Neotropical fishes*. Porto Alegre: EDIPUCRS, 171–192.

Weitzman SH, Menezes NA, Evers H-G, Burns JR. 2005. Putative relationships among inseminating and externally fertilizing characids, with a description of a new genus and species of Brazilian inseminating fish bearing an anal-fin gland in males (Characiformes: Characidae). *Neotropical Ichthyology* **3:** 329–360.

Winterbottom R. 1973. A descriptive synonymy of the striated muscles of the Teleostei. *Proceedings of the Academy of Natural Sciences of Philadelphia* **125:** 225–317.

Zanata AM, Vari RP. 2005. The family Alestidae (Ostariophysi, Characiformes): a phylogenetic analysis of a trans-Atlantic clade. *Zoological Journal of the Linnean Society* **145:** 1–144.

SUPPORTING INFORMATION

Additional supporting information may be found in the online version of this article at the publisher's web-site:

Appendix S1. List of examined specimens.
Appendix S2. List of 120 terminal taxa coded for the 157 added characters.
Appendix S3. Character list.
Appendix S4. Data matrix.
Appendix S5. Results of the explored parameters under the IW method.
Appendix S6. Full version of the IW consensus used as the final hypothesis.
Appendix S7. Full list of common synapomorphies obtained in the trees used to construct the final hypothesis.
Appendix S8. List of measures of character fit.